Evaluation and Application of Existing Air Curtain Effectiveness Methodology

Liangzhu (Leon) Wang, David A. Johnson, and Frank Cuaderno

Nomenclature

A — Area
A_i — Door section area of the ith section
b_0 — Air curtain nozzle depth
b_v — Nozzle depth of the virtual air curtain
C_A — Airflow coefficient
C_D — Discharge coefficient
$C_{D,ac}$ — Average discharge coefficient for each door operation section
D — The distance from the test point to the discharge nozzle
D_v — The distance from the test point to the virtual nozzle
$D_{D,ac}$ — Discharge modifier (air curtains)
H — Door height
H_v — Door height of the virtual air curtain
q — Representative flow rate
q_i — Representative flow rate of the ith section
q_h — Representative flow rate at the air curtain level
q_l — Representative flow rate at the ground level
Q — Volume flow rate
Q_{AC} — Total volume flow rate with the air curtain installed
Q_{ACi} — Volume flow rate of the ith section
Q_{SD} — Volume flow rate of the single door
ΔP_{oi} — Pressure difference across the air curtain doors
u — Airflow velocity
u_0 — Discharge velocity
u_{0i} — Average discharge velocity of the ith nozzle section
u_E — Equivalent discharge velocity
u_{Ei} — Equivalent discharge velocity of the ith nozzle section
u_{testi} — Measured airflow velocity of the ith section
u_v — Discharge velocity of the virtual air curtain

L. (Leon) Wang · D. A. Johnson (✉) · F. Cuaderno
Berner International LLC, New Castle, PA, USA
e-mail: leon.wang@concordia.ca; djohnson@berner.com; Frankc@marsair.com

W Door width
w_i Section width of the ith section
x Distance to the air curtain
θ Air curtain discharge angle
ρ Air density
$\eta_{\left(\frac{AC}{SD}\right)}$ Efficiency factor

1 Introduction

Air infiltration and exfiltration through building entrance doors may contribute to a large part of building heating and cooling loads. In previous studies, the operational characteristics of air curtain units were investigated and the potential in energy saving was justified ([4, 5, 6, 15, 16]). The airflow patterns of the air curtain jet under different pressure differences could be categorized into three working conditions: inflow breakthrough (IB), outflow breakthrough (OB), and optimum condition (OC) [7, 13–16], corresponding to the different performances of blocking the infiltration/exfiltration between indoor and outdoor environments.

The infiltration/exfiltration flow rate reflects the sealing effectiveness of air curtain units [2, 6, 10, 11]. However, there is no efficiency evaluation method that is convenient enough to obtain the infiltration/exfiltration information through door openings. Current air curtain efficiency rating method used in Europe requires a full-scale testing in an environmental chamber [3, 8] involving a series of well-controlled test conditions, such as chamber temperature, pressure, fan power, etc. The infiltration/exfiltration flow rate through the test chamber door opening is measured to obtain the efficiency factor of the air curtain based on the test sensors. Meanwhile, another air curtain test method proposed by American National Standards Institute/Air Movement and Control Association (ANSI/AMCA) Standard 220-05 [1] or International Organization for Standardization (ISO) Standard 27327-1:2009 [12] is focused on the aerodynamic performance in terms of airflow velocity and uniformity. Without the need of the climate chamber testing, a test can be conducted in a common environment, so it is relatively simpler than the European method. However, there is a lack of method that can relate the ANSI/AMCA or ISO Standards velocity test results to the infiltration/exfiltration rate and the air curtain efficiency. If the aerodynamic performance and the infiltration rate can be related directly, the ANSI/AMCA or ISO aerodynamic test method could be directly applied to the efficiency rating, which significantly reduces the cost of testing and rating while promoting a widely accepted standardized test methodology.

In this study, the relationships between the infiltration/exfiltration rates and the pressure differences for different air curtain discharge velocities are explored and correlated based on multiple computational fluid dynamic (CFD) simulation results. A novel method to relate the air curtain aerodynamic performance data to its effectiveness was developed for the calculation of the air curtain efficiency factor.

In Sect. 2, the details and the procedure of this method are explained. Section 3 demonstrates the whole procedure by three case studies. Section 4 elaborates the validation method and the results. Finally, the conclusions and limitations of the current study are outlined in Sect. 5.

2   The Efficiency Factor Calculation Methods

2.1   *The Method for Door Height Within 3 Meters*

The air curtain effectiveness is often assessed by the efficiency factor $\eta_{\left(\frac{AC}{SD}\right)}$ (Eq. 1) [6] based on the ratio of the flow rate through the door opening with the air curtain (i.e., air curtain door), and without the air curtain installed (i.e., single door). The single-door flow rate Q_{SD} can be estimated by the model (Eq. 2) proposed by Yuill [17, 18] dependent on the door size and the pressure difference. It is common that the discharge coefficient for the single door, $C_D = 0.65$. For the air curtain door, the infiltration rate Q_{AC} may also depend on the air curtain jet properties. Note that hereafter, the infiltration and the infiltration/exfiltration are used interchangeably if not specified. Wang and Zhong [15, 16] developed the air curtain infiltration/exfiltration model by adding a modifier coefficient $D_{D,AC}$ (Eq. 3) to Eq. 2. The coefficients in the model, $C_{D,AC}$ and $D_{D,AC}$, can be characterized by experiments or simulation results.

$$\eta_{\left(\frac{AC}{SD}\right)} = 1 - \frac{|Q_{AC}|}{|Q_{SD}|} \tag{1}$$

$$Q_{SD} = C_D A \sqrt{\frac{2\Delta P_{oi}}{\rho}} \tag{2}$$

$$\frac{Q_{AC}}{A\sqrt{2/\rho}} = sign\left(\Delta P_{oi}\right) C_{D,AC} \sqrt{|\Delta P_{oi}|} + D_{D,AC} \tag{3}$$

The proposed air curtain effectiveness rating method estimates the infiltration rates from the aerodynamic performance measurement data to determine the air curtain effectiveness for various design parameters, for example, discharge velocity u_0, nozzle depth b_0, discharge angle α, and door height H.

The discharge velocities of the nozzle sections are directly related to the capability of the air curtain to protect the corresponding door sections against the indoor and outdoor pressure differences. Following ANSI/AMCA Standard 220-05 [1] or ISO Standard 27327-1:2009 [12], if x is the coordinate direction along the jet flow centerline and y is the distance to the centerline in the plane perpendicular to the x-axis, the centerline peak velocity $u_{test,i}$ ($y = 0$) from a distance D to the nozzle sections can be measured (Fig. 1).
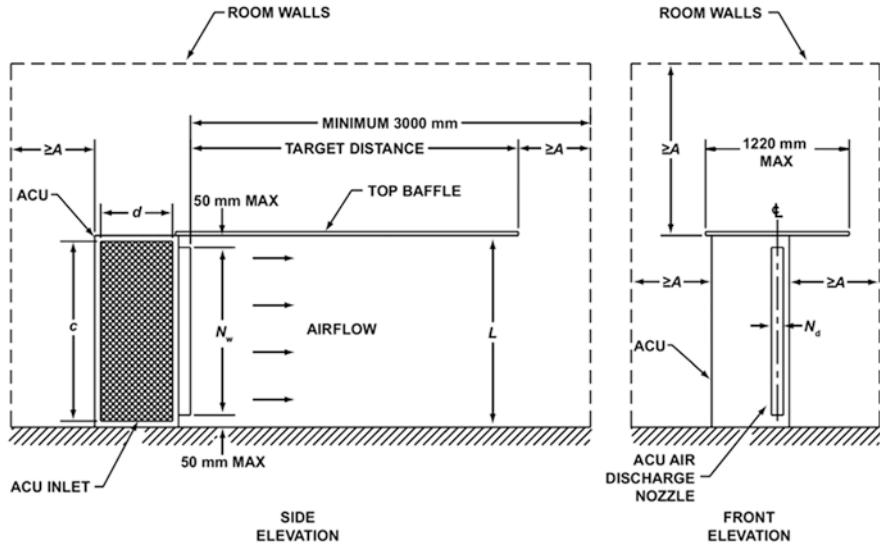
**Fig. 1** Aerodynamic test setup specified in ANSI/AMCA Standard 220-05 [1]

In the standard, the air curtain vanes are adjusted to an angle of 15° (Fig. 2b). In comparison, the proposed aerodynamic test by this study is slightly different, which requires the discharge angle to be 0° (Fig. 2a).

The reason is that the proposed method needs to calculate air curtain discharge velocities based on the jet theory, which has nothing to do with the jet angle. In other words, this study assumes that the air curtain jet follows the jet theory equation (Eq. 4) in the fully developed zone ($x > 5.2\, b_0$) [9]. Using the measured velocity distribution for the setup in Fig. 2a following the ANSI/AMCA Standard 220-05 or ISO 27327-1:2009, we can back-calculate (or inversely calculate) the average discharge velocity of each nozzle section $u_{0,i}$ (Eq. 5).

$$\frac{u}{u_0} = \frac{\sqrt{3}}{2}\sqrt{\frac{b_0\sigma_2}{x}}\left[1 - \tan h^2\left(\sigma_2\frac{y}{x}\right)\right], x > 5.2b_0, \sigma_2 = 7.67 \tag{4}$$

$$\frac{u_{\text{test},i}}{u_{0,i}} = \frac{\sqrt{3}}{2}\sqrt{\frac{b_0\sigma_2}{x}}, y = 0, \sigma_2 = 7.67, x = H \tag{5}$$

When the air curtain discharge velocity for each section is known, it is then possible to determine the corresponding air curtain door infiltration/exfiltration rate, Q, based on a series of standard air curtain Q-ΔP curves. These figures are obtained using the existing experimental and numerical simulation studies of previous air curtain studies, which cover a wide range of pressure differences and typical discharge velocities and angles. For a given air curtain unit with known discharge velocity and angle, and operating pressure difference, the infiltration/exfiltration

a)

Set the discharge angle $\theta = 0°$ (the vanes and jet direction perpendicular to the nozzle). The test lines parallel to the nozzle, also perpendicular to the jet direction.
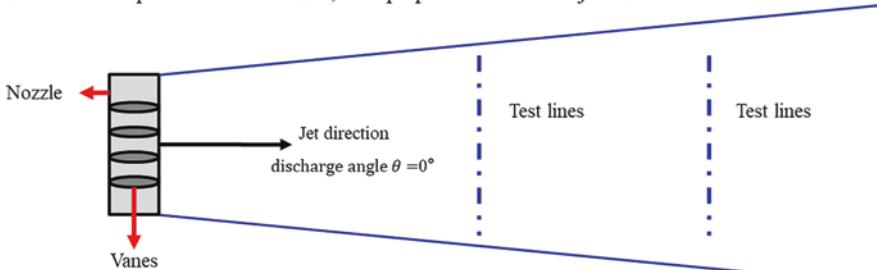
b)

Set the discharge angle $\theta = 15°$. The test lines parallel to the nozzle.
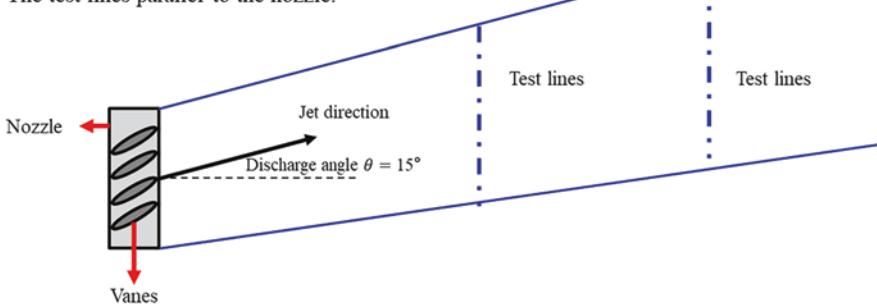
Fig. 2 Difference of the top views of (**a**) the proposed aerodynamic test in this method and (**b**) the method in ANSI/AMCA Standard 220-05 [1]

flow rate values for the air curtain can then be interpolated among these curves. The air curtain efficiency factor can then be evaluated using Eq. 1.

In this report, the scenarios of three typical discharge angles (0°, 10°, 20°), two nozzle depths (0.08 m and 0.10 m), and two door heights (2.4 m and 3 m) are considered as listed in Table 1 and the typical Q-ΔP curve figures are provided in the Appendix A. The figures for a 0.71 m height door, nozzle depth 0.0635 m, and 20° discharge angle were generated by previous research data for the validation of the proposed method.

When an air curtain supply nozzle is separated into n sections and the width of the ith ($i = 1~n$) section is w_i, each nozzle section is supposed to protect a corresponding door section below with an area of $A_i = Hw_i$. Therefore, an important step is to relate the area-averaged infiltration rates of the sections to their calculated discharge velocities. The typical Q-ΔP curves have been adjusted with a representative flow rate q as defined in Eq. 6a and substituted for the volumetric flow rate Q in Fig. 3. After the value of q_i for each air curtain subsection is interpolated, the infiltration rate of the door sections can be calculated by Eq. 6b. For this study, only

Table 1 List of the typical Q- ΔP curve figures

Discharge angle (°)	Nozzle depth (m)	Door height (m)	Figure index
20	0.0635	0.71	Case [20, 0.0635, 0.71] (for validation)
0	0.08	2.40	Case [0, 0.08, 2.4]
		3.00	Case [0, 0.08, 3.0]
	0.10	2.40	Case [0, 0.10, 2.4]
		3.00	Case [0, 0.10, 3.0]
10	0.08	2.40	Case [10, 0.08, 2.4]
		3.00	Case [10, 0.08, 3.0]
	0.10	2.40	Case [10, 0.10, 2.4]
		3.00	Case [10, 0.10, 3.0]
20	0.08	2.40	Case [20, 0.08, 2.4]
		3.00	Case [20, 0.08, 3.0]
	0.10	2.40	Case [20, 0.10, 2.4]
		3.00	Case [20, 0.10, 3.0]
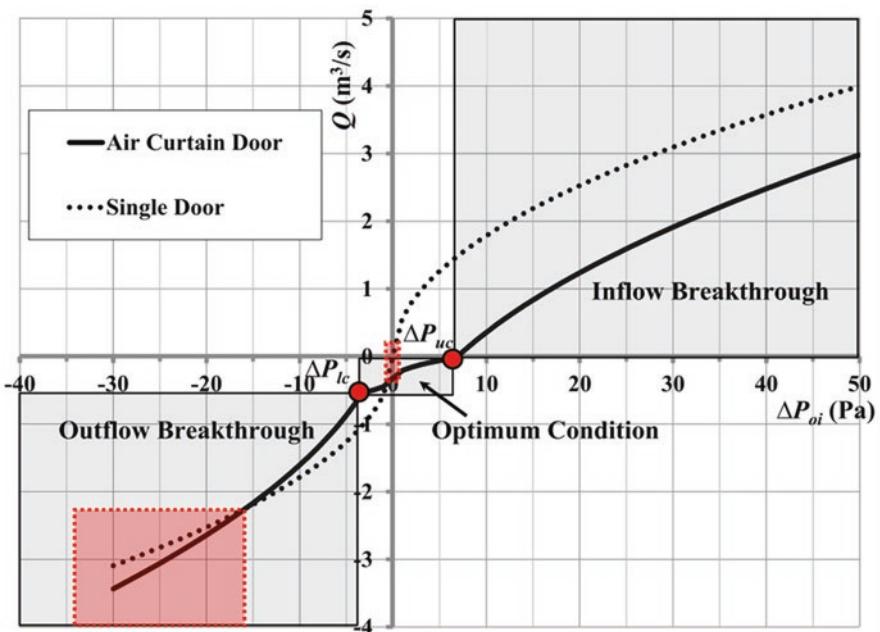
Fig. 3 Typical Q- ΔP curves in Goubran, et al. [7]

isothermal situation is investigated so the air density is considered a constant (1.2 kg/m³). Finally, the total airflow rate can be calculated by the sum of all the door sections (Eq. 7).

$$q = \frac{Q_{AC}}{A_i \sqrt{\dfrac{2}{\rho}}} \tag{6a}$$

$$Q_{AC,i} = A_i \sqrt{\frac{2}{\rho}} \, q_i \tag{6b}$$

$$Q_{AC} = \sum_{i=1}^{n} Q_{AC,i} \tag{7}$$

In summary, the five-step procedure to calculate the efficiency factor is as follows:

1. Separate the discharge nozzle into multiple sections and perform the aerodynamic test following ANSI/AMCA Standard 220-05 or ISO 27327-1:2009 to measure the jet flow distribution, $u_{test, i}$.
2. Calculate the discharge velocity $u_{0, i}$ for each section based on the measured velocity and the jet theory (Eq. 5).
3. Determine the representative flow rate q_i for each nozzle section from the standard Q- ΔP curves in Appendix A.
4. Calculate the infiltration rate for each door section $Q_{AC, i}$ (Eq. 6), then sum them up to obtain the total airflow rate through the door Q_{AC} (Eq. 7); and calculate the infiltration rate for the corresponding single door, Q_{SD}, by Eq. 2.
5. Calculate the efficiency factor, $\eta_{\left(\frac{AC}{SD}\right)}$, (Eq. 1).

2.2   The Method for Door Height over Three Meters

In our proposed method, the important step is to determine the representative flow rate q by the standard Q- ΔP curves. Normally, a standard figure for the Q- ΔP curve is used for a specified series of products that share the similar parameters (nozzle depth b_0, discharge angle α, and door height H). The specific scenarios in this report are listed in Table 1, limited to the door height of less than three meters. To apply these standard Q- ΔP figures for the door height more than three meters, we proposed a new method based on the concept of the equivalent air curtain model as explained in Fig. 4.

In an actual situation, the jet flow degrades and diverges gradually with the distance from the air curtain nozzle, implying that most of the infiltration/exfiltration, if any, should occur near the ground level rather than the higher level: that is, $q_h < q_l$.

For a door height more than three meters, if we follow the proposed method in the previous section (Fig. 4a), we need to determine q_i (Eq. 6), which is the
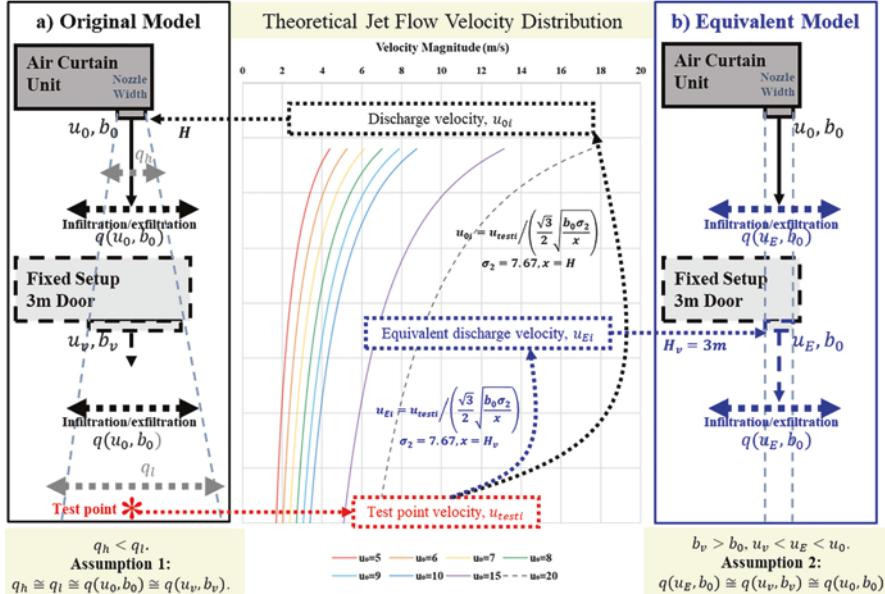
Fig. 4 (**a**) The original model and (**b**) the equivalent model for more than 3 m door height

area-averaged infiltration/exfiltration rate. The existing standard figures are based on the door height of three meters or less. For the door height over three meters, it is possible to assume that a virtual air curtain with the nozzle depth b_0 is located at the height of three meters above the floor (the equivalent model in Fig. 4b). This assumption is reasonable since for a typical air curtain, most of the infiltration/exfiltration occurs near the floor. Then, a similar five-step procedure as in Sect. 2.1 can be applied to the door higher than three meters with the following two assumptions:

1. The virtual air curtain located at 3-m height from the floor is with the nozzle depth of b_0 and the equivalent discharge velocity u_E.
2. The area-averaged infiltration rate, q_i, through the 3-m-height door section with the virtual air curtain is the same as that of the whole-door section with the actual air curtain unit.

Accordingly, the second and the third steps of the five-step procedure in Sect. 2.1 should be adjusted. In the second step, after the nozzle section is separated, the equivalent discharge velocity u_E at 3-m height should be calculated using the nozzle depth b_0 instead of the actual air curtain depth at the same height, b_v. For the third step, the standard figures for 3-m-high door should be used for the interpolation of the equivalent flow rate q_i, with the exception that the actual door height H should be used for the calculation of the total door section infiltration rate $Q_{AC, i}$ and the single-door flow rate Q_{SD}.

2.3 Resulting Calculation Procedure of Efficiency Factor

The methods are illustrated by the flowchart in Fig. 5. Note the velocity distribution is measured at the objective distance, that is, at the floor level: H (the door height) from the nozzle. For the equivalent model, the distance to the virtual air curtain unit is always 3 m. When there is no standard figure available, the existing standard figures close to the design parameters should be used by either interpolations or extrapolations.
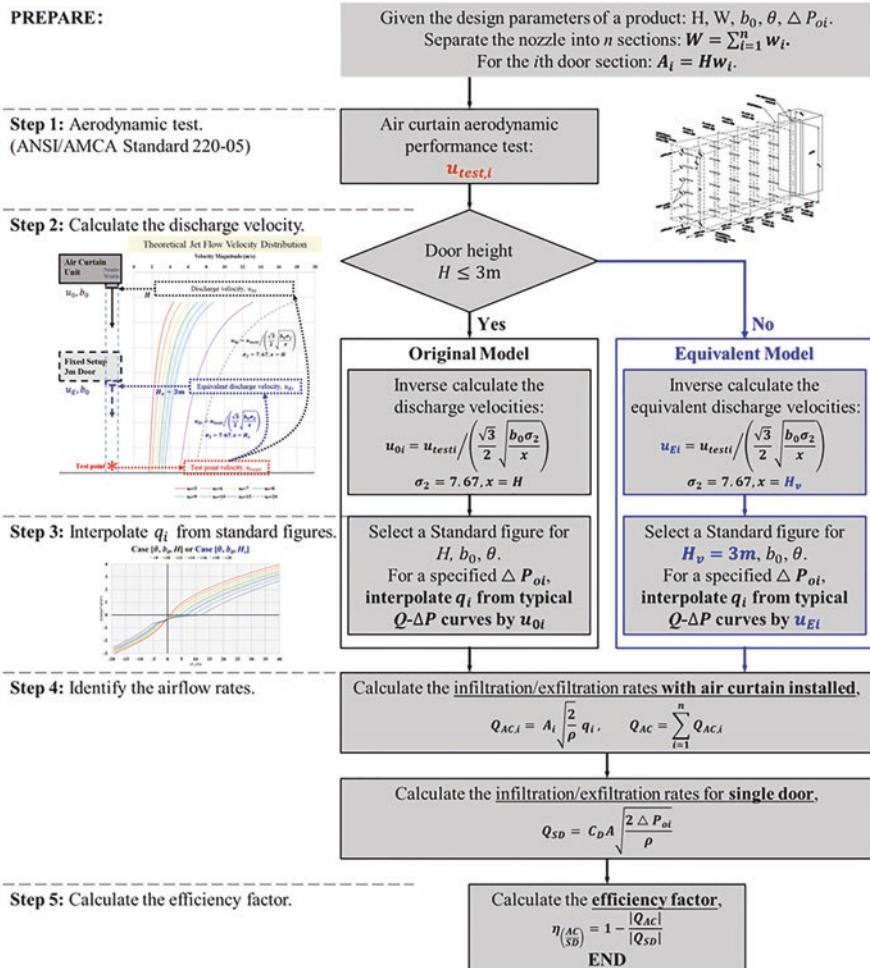
Fig. 5 Flowchart illustrating the procedure to calculate the efficiency factor

3   Case Studies and Discussions

In this section, three case studies are conducted to demonstrate the proposed efficiency factor calculation method. The first case study is for ordinary scenarios where the door height is within 3 m and corresponding standard figures are available; thus the procedure of calculation follows the original model in the flowchart in Fig. 5. The second and third case studies are for scenarios of door height more than 3 m; thus an estimation of the efficiency factor can only be carried out through the equivalent method by using the provided standard figures for 3 m doors.

The air curtain work conditions can be classified into three categories: the inflow breakthrough, optimum condition, and outflow breakthrough (Fig. 3). This classification is only based on the airflow rate through the door opening and the overall pattern of the air curtain jets. When it comes to the efficiency factor, as is defined by Eq. 1, the ratio of the absolute value of the infiltration/exfiltration flow rate with and without an air curtain installed matters. The distribution of the efficiency factor with the pressure difference will follow the theoretical pattern in Fig. 6. Some negative efficiency factor may occur in the outflow breakthrough and optimum conditions, respectively (Fig. 6). The negative efficiency factor values indicate that air curtain will have more exfiltration than single door. From considering a real-life scenario and mass balance, the exfiltration due to air curtain ought to be replaced from another source. With this concept, the correction to the $\eta_{air\left(\frac{AC}{SD}\right)}$ was made as shown by the corrected curve (i.e., dashed lines) in Fig. 6.

When the pressure difference is large enough to bend the main part of the air curtain jet, a CFD analysis shows that the air curtain jet may cause more airflow exfiltration rate through the door (Fig. 7). This phenomenon can be illustrated by the left red region in Figs. 3 and 6.

When the pressure difference is close to 0 Pa (the central red region in Figs. 3 and 6), the single-door infiltration/exfiltration flow rate is close to zero, and the corresponding efficiency factor defined by Eq. 1 would tend to become the infinity. This
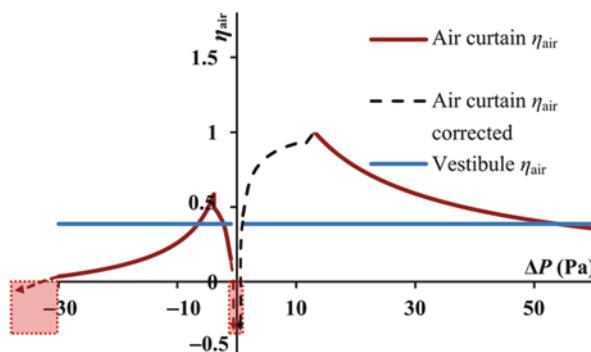
Fig. 6 Theoretical efficiency factor value distribution with different pressure difference [6]
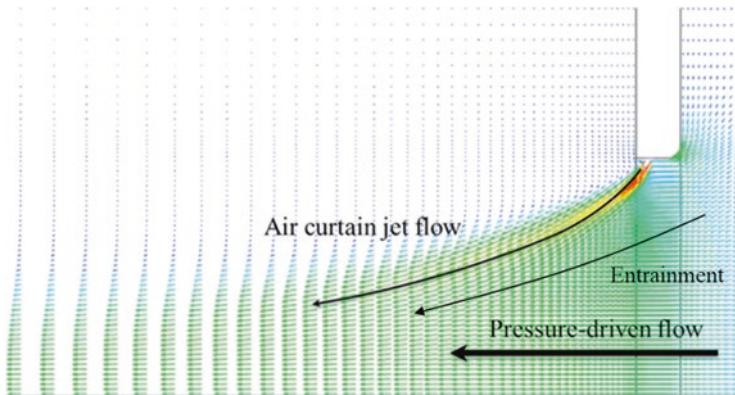
Fig. 7 Airflow pattern of fully outflow region

means that the efficiency factor in Eq. 1 becomes meaningless and trivial for this region.

3.1 Case 1: An Air Curtain for 2.4 m Door

The proposed method is demonstrated for an actual commercially available air curtain unit identified as Model A. In this case, the air curtain has a nozzle width of 1.98 m and a depth of 0.08 m, a discharge angle of 20° outward, and is designed for installation on a 2.4-m-high door.

Multiple CFD simulations were conducted to obtain the typical Q- ΔP curves, as shown in Fig. 3 based on the leakage model for air curtains (Eq. 3), for seven discharge velocities from 8 m/s to 20 m/s. The air curtain nozzle is separated into 20 sections. The width of the nozzle sections and the corresponding door sections are listed in Table 2.

In the first step, the velocity distributions at 2 m from the nozzle were measured ranging from 3.47 m/s to 4.84 m/s. Please note that the velocity distribution data provided from the manufacturer are only available up to 2 m instead of the door height of 2.4 m. Therefore, the current calculation is based on the velocity at 2 m. It is also recommended that when applying the method developed in this report, to avoid interpolations/extrapolations, the velocity distribution measurements should be available at least up to the door height where an air curtain is intended to be installed. In the second step, the corresponding discharge velocity for each section was calculated according to the jet theory in Eq. 5, where the distance x from the test points to the nozzle is 2 m. In the third step, it requires to identify the representative infiltration rates q value from the modified typical Q- ΔP curves. The discharge velocities of the sections in this case are in the range of 7.2 m/s and 10.1 m/s, so only

Table 2 Average flow rates of each nozzle section for Model A

Section number	Measured velocity (m/s)	u_0 (m/s)	Nozzle section width (m)	Door section area (m²)	Average flow rate q_i (Pa$^{0.5}$) for different pressure differences				
					25 Pa	9 Pa	1 Pa	−1 Pa	−9 Pa
1	4.84	10.1	0.1275	0.306	2.64	1.10	−0.15	−0.53	−2.03
2	4.11	8.6	0.095	0.228	2.81	1.31	−0.10	−0.58	−2.06
3	4.02	8.4	0.095	0.228	2.84	1.34	−0.09	−0.59	−2.07
4	4.53	9.4	0.0975	0.234	2.72	1.20	−0.12	−0.56	−2.05
5	4.27	8.9	0.0975	0.234	2.78	1.27	−0.11	−0.57	−2.06
6	3.89	8.1	0.095	0.228	2.87	1.38	−0.08	−0.60	−2.08
7	4.04	8.4	0.095	0.228	2.84	1.34	−0.09	−0.59	−2.07
8	4.4	9.2	0.095	0.228	2.75	1.22	−0.12	−0.56	−2.05
9	3.79	7.9	0.095	0.228	2.89	1.40	−0.08	−0.61	−2.08
10	4.1	8.5	0.0975	0.234	2.83	1.32	−0.10	−0.59	−2.07
11	3.84	8.0	0.0975	0.234	2.88	1.39	−0.08	−0.61	−2.08
12	4.49	9.4	0.095	0.228	2.72	1.20	−0.12	−0.56	−2.05
13	3.75	7.8	0.095	0.228	2.91	1.42	−0.08	−0.61	−2.08
14	4.37	9.1	0.095	0.228	2.76	1.24	−0.12	−0.57	−2.05
15	3.86	8.0	0.095	0.228	2.88	1.39	−0.08	−0.61	−2.08
16	4.02	8.4	0.0975	0.234	2.84	1.34	−0.09	−0.59	−2.07
17	3.9	8.1	0.0975	0.234	2.87	1.38	−0.08	−0.60	−2.08
18	4.17	8.7	0.095	0.228	2.80	1.29	−0.10	−0.58	−2.06
19	3.47	7.2	0.095	0.228	2.97	1.50	−0.06	−0.63	−2.10
20	3.94	8.2	0.1075	0.258	2.86	1.36	−0.09	−0.60	−2.07
Total value			1.96	4.704					

the curves of 8 m/s, 10 m/s, and 12 m/s in Fig. 17 were used for the calculation of q_i. The results for these three steps are shown in Table 2.

In the fourth step, the airflow rate through each door section $Q_{AC, i}$ can be calculated according to the door section areas and the local air density. By summing up the volumetric flow rate through each door section, the total airflow rates Q_{AC} are calculated to be 16.96 m³/s, 7.90 m³/s, –0.59 m³/s, –3.52 m³/s, and –12.42 m³/s under the pressure difference of 25 Pa, 9 Pa, 1 Pa, –1 Pa, and –9 Pa, respectively. For the pressure difference of –9 Pa, the airflow rate with an air curtain may exceed that of a single door, which is only –11.72 m³/s. The air exchange rate Q_{SD} of a single door is calculated by Eq. 2.

Finally, the efficiency factor $\eta_{\left(\frac{AC}{SD}\right)}$ can be found using Eq. 1. The results show that this air curtain unit has the ability to block 13% infiltration for the 25 Pa pressure difference, and 33% at 9 Pa pressure difference. The best efficiency is achieved for 1 Pa with 85%. For –1 Pa and –9 Pa, the corresponding efficiency factor reduced to 10% and –6%, respectively. The air curtain may step into the negative efficiency at the pressure difference of –9 Pa (Fig. 7). This is an example to show that, for a large outward discharge angle (20°), the air curtain can still perform well to separate

Table 3 Volume flow rate through the door and the air curtain efficiency for Mode A

Section number	u_0 (m/s)	Volume flow rate Q_i m³/s under different pressure differences				
		25 Pa	9 Pa	1 Pa	−1 Pa	−9 Pa
1	10.10	1.03	0.43	−0.06	−0.21	−0.79
2	8.60	0.82	0.38	−0.03	−0.17	−0.60
3	8.40	0.83	0.39	−0.03	−0.17	−0.60
4	9.40	0.81	0.36	−0.04	−0.17	−0.61
5	8.90	0.83	0.38	−0.03	−0.17	−0.62
6	8.10	0.84	0.40	−0.02	−0.18	−0.60
7	8.40	0.83	0.39	−0.03	−0.17	−0.60
8	9.20	0.80	0.36	−0.03	−0.16	−0.60
9	7.90	0.84	0.41	−0.02	−0.18	−0.61
10	8.50	0.85	0.40	−0.03	−0.18	−0.62
11	8.00	0.86	0.42	−0.02	−0.18	−0.62
12	9.40	0.79	0.35	−0.04	−0.16	−0.60
13	7.80	0.85	0.41	−0.02	−0.18	−0.61
14	9.10	0.80	0.36	−0.03	−0.16	−0.60
15	8.00	0.84	0.41	−0.02	−0.18	−0.61
16	8.40	0.85	0.40	−0.03	−0.18	−0.62
17	8.10	0.86	0.41	−0.03	−0.18	−0.62
18	8.70	0.82	0.38	−0.03	−0.17	−0.60
19	7.20	0.87	0.44	−0.02	−0.18	−0.61
20	8.20	0.94	0.45	−0.03	−0.20	−0.68
Total Q_{AC} m³/s		16.96	7.90	−0.59	−3.52	−12.42
Total Q_{SD} m³/s		19.53	11.72	3.91	−3.91	−11.72
Efficiency factor		0.13	0.33	0.85	0.10	−0.06

the indoor and outdoor environments when the outdoor pressure is much higher than indoor (25 Pa pressure difference), but this protection can be easily destroyed by a small negative pressure difference (−9 Pa). The results for the last two steps are shown in Table 3.

3.2 *Case 2: An Air Curtain for 5 m Door*

The air curtain unit described in Model B is designed for a 5-m-high door, with a nozzle width of 0.9 m and a depth of 0.08 m, and the discharge angle of 10° outward. The standard figures for door height of 3 m, nozzle depth of 0.08 m, and discharge angle of 10° were used for the calculation of q_i. The air curtain nozzle is separated into nine sections equally, with the nozzle section width of 0.1 m and the door section area of 0.5 m².

Table 4 lists the results of the first three steps. In the first step, the measured velocity distribution at five meters from the nozzle was from 3.56 m/s to 4.57 m/s following the standard. In the second step, the corresponding equivalent discharge velocities at 3 m for each section were calculated to be in the range of 9.08 m/s and 11.67m/s according to the jet theory in Eq. 5. In the third step, the typical Q- ΔP curves in Fig. 21 for 3 m door are used for the interpolation of q_i for each nozzle section.

Table 5 summarizes the results of steps 4 and 5. In the fourth step, the airflow rates through each door section $Q_{AC, i}$ are calculated according to the real door section areas (0.5 m²). By summing up the volumetric flow rate through each door section, the total airflow rates Q_{AC} are calculated to be 16.58 m³/s, 8.00 m³/s, –0.04 m³/s, –2.43 m³/s, and –11.11m³/s under the pressure difference of 25 Pa, 9 Pa, 1 Pa, –1 Pa, and –9 Pa, respectively. The air exchange rate Q_{SD} of a single door is calculated by Eq. 2 using the real door size (4.5 m²). In the fifth step, the efficiency factor $\eta\left(\frac{AC}{SD}\right)$ can be calculated by Eq. 1. The results show that this air curtain unit has the ability to block 11% infiltration for the 25 Pa pressure difference, and 29% at 9 Pa pressure difference. The best efficiency is also achieved for 1 Pa with 99%. For –1 Pa and –9 Pa, the corresponding efficiency factor reduced to 35% and 1%, respectively.

3.3 Case 3: An Air Curtain for 8 m Door

The air curtain unit Model C is designed for an 8-m-high door, with a nozzle width of 2.4 m, a depth of 0.2 m, and a discharge angle of 15° outward. As the size of this air curtain is too large for the aerodynamic test, it is separated into three modules equally along the nozzle width. Each of them has a nozzle width of 0.8 m. The

Table 4 Average flow rates of each nozzle section for Model B

Section number	Measured velocity (m/s)	Equivalent u_E (m/s)	Nozzle section width (m)	Door section area (m²)	Average flow rate q_i Pa$^{0.5}$ for different pressure differences				
					25 Pa	9 Pa	1 Pa	−1 Pa	−9 Pa
1	4.32	11.02	0.1	0.5	2.82	1.33	−0.03	−0.39	−1.91
2	4.06	10.38	0.1	0.5	2.88	1.39	−0.02	−0.42	−1.93
3	4.06	10.38	0.1	0.5	2.88	1.39	−0.02	−0.42	−1.93
4	3.56	9.08	0.1	0.5	2.98	1.50	0.04	−0.48	−1.98
5	3.81	9.73	0.1	0.5	2.93	1.44	0.00	−0.45	−1.96
6	3.56	9.08	0.1	0.5	2.98	1.50	0.04	−0.48	−1.98
7	3.81	9.73	0.1	0.5	2.93	1.44	0.00	−0.45	−1.96
8	4.57	11.67	0.1	0.5	2.77	1.27	−0.04	−0.35	−1.88
9	4.57	11.67	0.1	0.5	2.77	1.27	−0.04	−0.35	−1.88
Total value			0.9	4.5					

nozzle partitioning method and the dimensions of nozzle sections are illustrated in Fig. 8. The three modules have been further separated into five nozzle sections in the same way according to the standard, and the test results for each module are the same. For the whole air curtain nozzle, there are 15 sections in total, among which sections 1, 5, 6, 10, 11, and 15 have a section width of 0.28 m (door section area 2.24 m²), and the rest of them 0.08 m (door section area 0.64 m²). Because the test results and the dimensions of each module are the same, the efficiency factor of the whole unit is the same with one of the modules. Therefore, the calculation procedure demonstrated below will be carried out for only one module and the results of the efficiency factors can represent for the whole unit.

The velocity distribution data at 8 m to the nozzle are used for the calculation. The calculation procedure is demonstrated in Fig. 9. Since the nozzle depth of this unit is 0.2 m, the airflow rate calculation will be performed twice for the nozzle depth of both 0.08 m and 0.1 m, and then followed by an extrapolation process to

Table 5 Volume flow rate through the door and the air curtain efficiency for Model B

Section number	Equivalent u_E (m/s)	Volume flow rate Q_i m³/s under different pressure differences				
		25 Pa	9 Pa	1 Pa	−1 Pa	−9 Pa
1	11.02	1.80	0.85	−0.02	−0.25	−1.22
2	10.38	1.84	0.89	−0.01	−0.27	−1.23
3	10.38	1.84	0.89	−0.01	−0.27	−1.23
4	9.08	1.90	0.96	0.03	−0.31	−1.26
5	9.73	1.87	0.92	0.00	−0.29	−1.25
6	9.08	1.90	0.96	0.03	−0.31	−1.26
7	9.73	1.87	0.92	0.00	−0.29	−1.25
8	11.67	1.77	0.81	−0.03	−0.23	−1.20
9	11.67	1.77	0.81	−0.03	−0.23	−1.20
Total Q_{AC} m³/s		16.58	8.00	−0.04	−2.43	−11.11
Total Q_{SD} m³/s		18.69	11.21	3.74	−3.74	−11.21
Efficiency factor		0.11	0.29	0.99	0.35	0.01
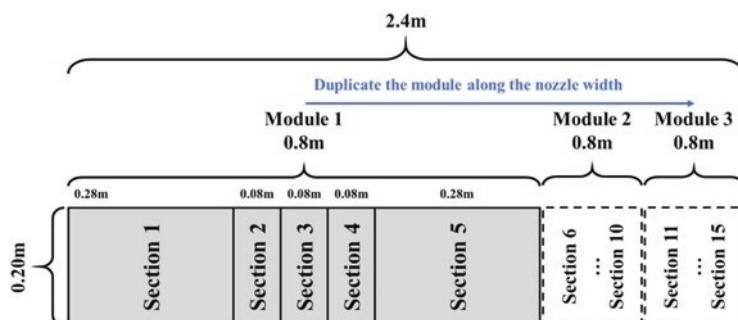
Fig. 8 Dimensions of Model C and the nozzle partitioning method in the aerodynamic test
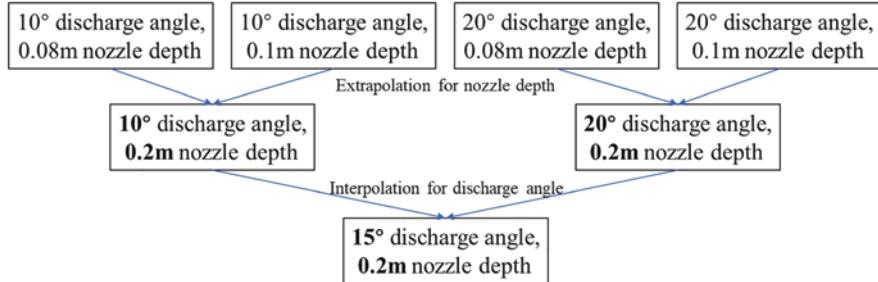
Fig. 9 Procedure to calculate three discharge angles for a nozzle depth of 0.2 m

calculate for the nozzle depth of 0.2 m. The discharge angles of 10° and 20° outward will be calculated directly from the provided standard figures, while the 15° outward calculation will be an interpolation by the results of the previous two discharge angles.

In the first step, the velocity distribution at 8 m to the air curtain nozzle is measured to be uniform, which is 7.62 m/s for all the nozzle sections. In the second step, the corresponding equivalent discharge velocities at 3-m height are calculated to be 19.46 m/s by the jet theory Eq. 5.

In the third step, the typical Q-ΔP curves in Figs. 21, 22, 23, and 24 are used for the identification of the representative flow rate q for the discharge angles of 10° (Tables 6 and 7) and 20° (Tables 8 and 9), respectively.

In the fourth step, the airflow rates through each door section $Q_{AC, i}$ for the two discharge angles and two nozzle depths are calculated according to the real door section areas (Tables 10, 11, 12, and 13).

In the final step, the airflow rates for the nozzle depth of 0.2 m are first extrapolated by the results of 0.1 m and 0.08 m, and then the airflow rates for discharge angle of 15° are interpolated by the results of 10° and 20°. The air exchange rate Q_{SD} of a single door is calculated by Eq. 2 using the real door size (6.4 m²). Thus, the efficiency factor can be calculated for the setup of 0.2 m nozzle depth and 15° discharge angle. The efficiency factors are 85%, 65%, –3%, –51%, and 43%. The best efficiencies for the three discharge angles are achieved for 25 Pa. When the pressure difference is 1 Pa and –1 Pa, the efficiency factor drops to negative at the near-zero pressure difference area as discussed in Fig. 6 (Tables 14, 15, and 16).

3.4 Discussions

In Case 1, the efficiency factors of the air curtain for door height of 2.4 m are calculated following the calculation procedure in Fig. 5 using the original model. In the other two cases, the door heights are more than 3 m, so the equivalent model is

Table 6 Average flow rates of each nozzle section for a module of Model C using the standard figure for 0.08 m nozzle depth, 10° discharge angle, and 3 m door

Section number	Measured velocity (m/s)	Equivalent u_E (m/s)	Nozzle section width (m)	Door section area (m²)	Average flow rate q_i Pa$^{0.5}$ for different pressure differences				
					25 Pa	9 Pa	1 Pa	−1 Pa	−9 Pa
1	7.62	19.46	0.28	2.24	1.87	0.12	−0.20	−0.42	−1.48
2	7.62	19.46	0.08	0.64	1.87	0.12	−0.20	−0.42	−1.48
3	7.62	19.46	0.08	0.64	1.87	0.12	−0.20	−0.42	−1.48
4	7.62	19.46	0.08	0.64	1.87	0.12	−0.20	−0.42	−1.48
5	7.62	19.46	0.28	2.24	1.87	0.12	−0.20	−0.42	−1.48
Total value			0.8	6.4					

Table 7 Average flow rates of each nozzle section for a module of Model C using the standard figure for 0.1 m nozzle depth, 10° discharge angle, and 3 m door

Section number	Measured velocity (m/s)	Equivalent u_E (m/s)	Nozzle section width (m)	Door section area (m²)	Average flow rate q_i Pa$^{0.5}$ for different pressure differences				
					25 Pa	9 Pa	1 Pa	−1 Pa	−9 Pa
1	7.62	19.46	0.28	2.24	1.52	−0.04	−0.27	−0.50	−1.32
2	7.62	19.46	0.08	0.64	1.52	−0.04	−0.27	−0.50	−1.32
3	7.62	19.46	0.08	0.64	1.52	−0.04	−0.27	−0.50	−1.32
4	7.62	19.46	0.08	0.64	1.52	−0.04	−0.27	−0.50	−1.32
5	7.62	19.46	0.28	2.24	1.52	−0.04	−0.27	−0.50	−1.32
Total value			0.8	6.4					

Table 8 Average flow rates of each nozzle section for a module of Model C using the standard figure for 0.08 m nozzle depth, 20° discharge angle, and 3 m door

Section number	Measured velocity (m/s)	Equivalent u_E (m/s)	Nozzle section width (m)	Door section area (m²)	Average flow rate q_i Pa$^{0.5}$ for different pressure differences				
					25 Pa	9 Pa	1 Pa	−1 Pa	−9 Pa
1	7.62	19.46	0.28	2.24	1.63	−0.01	−0.28	−0.53	−1.97
2	7.62	19.46	0.08	0.64	1.63	−0.01	−0.28	−0.53	−1.97
3	7.62	19.46	0.08	0.64	1.63	−0.01	−0.28	−0.53	−1.97
4	7.62	19.46	0.08	0.64	1.63	−0.01	−0.28	−0.53	−1.97
5	7.62	19.46	0.28	2.24	1.63	−0.01	−0.28	−0.53	−1.97
Total value			0.8	6.4					

Table 9 Average flow rates of each nozzle section for a module of Model C using the standard figure for 0.1 m nozzle depth, 20° discharge angle, and 3 m door

Section number	Measured velocity (m/s)	Equivalent u_E (m/s)	Nozzle section width (m)	Door section area (m²)	Average flow rate q_i Pa$^{0.5}$ for different pressure differences				
					25 Pa	9 Pa	1 Pa	−1 Pa	−9 Pa
1	7.62	19.46	0.28	2.24	1.24	−0.10	−0.36	−0.62	−1.92
2	7.62	19.46	0.08	0.64	1.24	−0.10	−0.36	−0.62	−1.92
3	7.62	19.46	0.08	0.64	1.24	−0.10	−0.36	−0.62	−1.92
4	7.62	19.46	0.08	0.64	1.24	−0.10	−0.36	−0.62	−1.92
5	7.62	19.46	0.28	2.24	1.24	−0.10	−0.36	−0.62	−1.92
Total value			0.4	3.2					

Table 10 Volume flow rate through the door and the air curtain efficiency for a module of Model C using the standard figure for 0.08 m nozzle depth, 10° discharge angle, and 3 m door

Section number	Equivalent u_E (m/s)	Volume flow rate Q_i m³/s under different pressure differences				
		25 Pa	9 Pa	1 Pa	−1 Pa	−9 Pa
1	19.46	5.36	0.35	−0.58	−1.21	−4.23
2	19.46	1.53	0.10	−0.17	−0.35	−1.21
3	19.46	1.53	0.10	−0.17	−0.35	−1.21
4	19.46	1.53	0.10	−0.17	−0.35	−1.21
5	19.46	5.36	0.35	−0.58	−1.21	−4.23
Total Q_{AC} m³/s		15.31	0.99	−1.67	−3.46	−12.09

Table 11 Volume flow rate through the door and the air curtain efficiency for a module of Model C using the standard figure for 0.1 m nozzle depth, 10° discharge angle, and 3 m door

Section number	Equivalent u_E (m/s)	Volume flow rate Q_i m³/s under different pressure differences				
		25 Pa	9 Pa	1 Pa	−1 Pa	−9 Pa
1	19.46	4.36	−0.11	−0.77	−1.43	−3.78
2	19.46	1.25	−0.03	−0.22	−0.41	−1.08
3	19.46	1.25	−0.03	−0.22	−0.41	−1.08
4	19.46	1.25	−0.03	−0.22	−0.41	−1.08
5	19.46	4.36	−0.11	−0.77	−1.43	−3.78
Total Q_{AC} m³/s		12.47	−0.32	−2.19	−4.07	−10.81

implemented. The standard figures are used for the interpolation of the q_i values for each door section, which cover a great number of scenarios.

In Case 3, the efficiency factor for 0.2 m nozzle depth and 15° discharge angle is not included in the provided standard figures. It is a well-demonstrated example to calculate by multiple interpolation and extrapolation operations of the other scenarios.

Table 12 Volume flow rate through the door and the air curtain efficiency for a module of Model C using the standard figure for 0.08 m nozzle depth, 20° discharge angle, and 3 m door

Section number	Equivalent u_E (m/s)	Volume flow rate Q_i m³/s under different pressure differences				
		25 Pa	9 Pa	1 Pa	−1 Pa	−9 Pa
1	19.46	4.68	−0.04	−0.80	−1.52	−5.63
2	19.46	1.34	−0.01	−0.23	−0.43	−1.61
3	19.46	1.34	−0.01	−0.23	−0.43	−1.61
4	19.46	1.34	−0.01	−0.23	−0.43	−1.61
5	19.46	4.68	−0.04	−0.80	−1.52	−5.63
Total Q_{AC} m³/s		13.36	−0.10	−2.29	−4.34	−16.09

Table 13 Volume flow rate through the door and the air curtain efficiency for a module of Model C using the standard figure for 0.1 m nozzle depth, 20° discharge angle, and 3 m door

Section number	Equivalent u_E (m/s)	Volume flow rate Q_i m³/s under different pressure differences				
		25 Pa	9 Pa	1 Pa	−1 Pa	−9 Pa
1	19.46	3.54	−0.27	−1.03	−1.79	−5.51
2	19.46	1.01	−0.08	−0.29	−0.51	−1.57
3	19.46	1.01	−0.08	−0.29	−0.51	−1.57
4	19.46	1.01	−0.08	−0.29	−0.51	−1.57
5	19.46	3.54	−0.27	−1.03	−1.79	−5.51
Total Q_{AC} m³/s		10.10	−0.78	−2.94	−5.11	−15.73

Table 14 Extrapolation for the 0.2 m nozzle depth with a discharge angle of 10°

Pressure difference (Pa)	25	9	1	−1	−9
Q_{ac} for 0.08 m nozzle depth (m³/s)	15.31	0.99	−1.67	−3.46	−12.09
Q_{ac} for 0.1 m nozzle depth (m³/s)	12.47	−0.32	−2.19	−4.07	−10.81
Q_{ac} for 0.2 m nozzle depth (m³/s)	−1.73	−6.87	−4.79	−7.12	−4.41

Table 15 Extrapolation for the 0.2 m nozzle depth with a discharge angle of 20°

Pressure difference (Pa)	25	9	1	−1	−9
Q_{ac} for 0.08 m nozzle depth (m³/s)	13.36	−0.1	−2.29	−4.34	−16.09
Q_{ac} for 0.1 m nozzle depth (m³/s)	10.1	−0.78	−2.94	−5.11	−15.73
Q_{ac} for 0.2 m nozzle depth (m³/s)	−6.20	−4.18	−6.19	−8.96	−13.93

Table 16 Interpolation for the 15° discharge angle by the results of 10° and 20°

Pressure difference (Pa)	25	9	1	−1	−9
Q_{ac} for 20° (m³/s)	−6.20	−4.18	−6.19	−8.96	−13.93
Q_{ac} for 10° (m³/s)	−1.73	−6.87	−4.79	−7.12	−4.41
Q_{ac} for 15° (m³/s)	−3.97	−5.53	−5.49	−8.04	−9.17
Q_{sd} (m³/s)	26.58	15.95	5.32	−5.32	−15.95
Efficiency factor	0.85	0.65	−0.03	−0.51	0.43

This report provides 12 standard figures with 7 curves of different velocities, covering a wide range of practical situations for many design scenarios by applying interpolations and/or extrapolations.

4 Validation of the Method

4.1 Validation Setup

To confirm the effectiveness of the new method, the results from the proposed method are compared with the experimental and simulation data from previous studies. The only factor affecting the efficiency factor calculation value is the infiltration/exfiltration flow rate, so the results are compared in terms of the flow rates. The configuration of the experiments and the simulations were elaborated by Goubran et al. [7]. The air curtain has a nozzle depth of 0.0635 m and an outward discharge angle of 20°. It was installed in the lab chamber with a door height and width of 0.71 m and 0.61 m, respectively. The CFD model used the User Defined Function (UDF) to specify the similar air curtain nozzle boundary condition based on the measured velocity profile. The typical Q-ΔP curves (Fig. 10) were prepared by setting the air curtain nozzle as the uniform velocity inlet in the simulation from 8 m/s to 18 m/s. Then, we can repeat the procedure as described in Sect. 2.1 to calculate the total airflow rates Q_{AC} through the door.
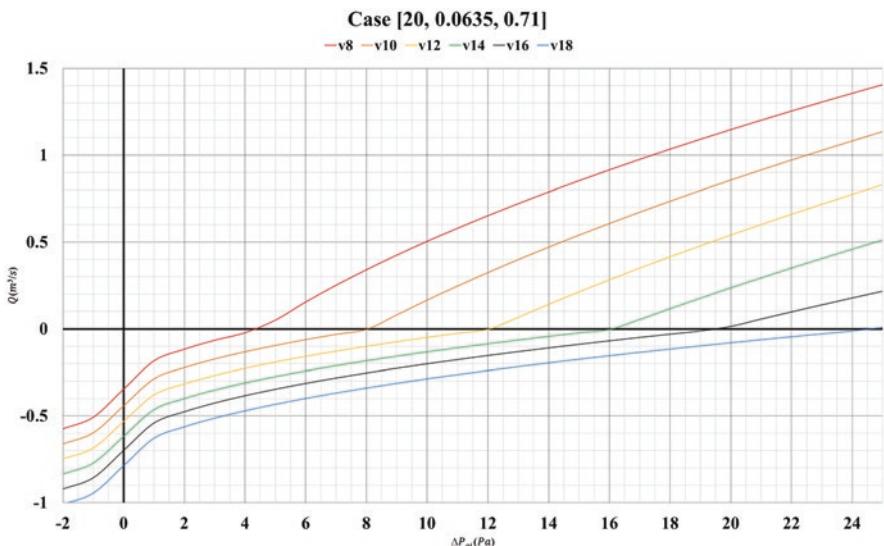
Fig. 10 The standard figure of the typical Q-ΔP curves for 0.71 m door, 0.0635 m nozzle depth, and discharge angle of 20°

The air curtain nozzle is separated into 12 sections. Each section has a width of 0.0508 m and the corresponding door section area is 0.036 m². Two average discharge velocities, 13.75 m/s and 9.1 m/s, were tested, and the measured discharge velocity distribution for each nozzle is listed in Table 17. The measured discharge velocities for each section were used to interpolate from Fig. 10; thus the corresponding representative flow rate q_i and the infiltration rate $Q_{AC, i}$ for different pressure differences can be obtained. By summing up the flow rates $Q_{AC, i}$ through all the door sections, the total airflow rates Q_{AC} through the opening are calculated.

4.2   Validation Results

The calculated airflow rates are compared in Fig. 11 with the previous results in Goubran et al. [7]. A good agreement between the previous CFD simulation data and the experimental data ensured validity of the CFD method. The new method extends the empirical infiltration model based on more CFD simulation results. Thus, it can well capture the trend for the inflow breakthrough condition and the optimum condition, and most of the points are located between the CFD data and the experimental data. Instead of considering the air curtain supply jet as a uniform airflow, the separation of the air curtain nozzle can partly conserve the airflow distribution along the door width.

Figure 12 exhibits the correlation of the proposed method with the experimental and CFD simulation data. The calculated flow rates by the method are close to both experimental and simulation data for the inflow breakthrough region. In the optimum condition, the jet flow reached the ground and caused some uncertainties for

Table 17   Section separation for the air curtain unit and measured discharge velocity

Section number	Section width (m)	Door section area (m²)	Discharge velocity average 13.75 m/s	Discharge velocity average 9.1 m/s
1	0.051	0.036	13.55	9.41
2	0.051	0.036	16.07	10.33
3	0.051	0.036	16.97	10.86
4	0.051	0.036	14.67	9.71
5	0.051	0.036	10.95	7.52
6	0.051	0.036	8.34	5.67
7	0.051	0.036	8.42	5.24
8	0.051	0.036	11.28	6.57
9	0.051	0.036	15.32	9.11
10	0.051	0.036	17.94	11.56
11	0.051	0.036	17.25	12.40
12	0.051	0.036	14.24	10.82
Nozzle width	0.61	0.43		
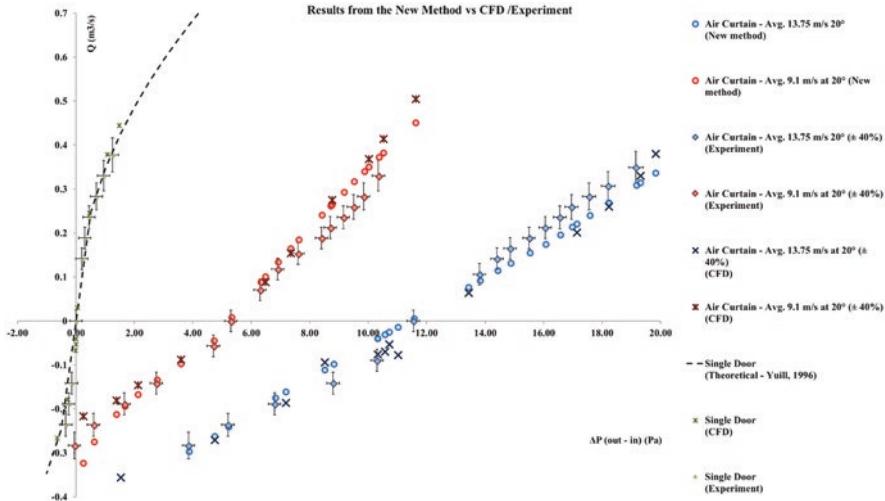
Fig. 11 Results comparison of the new method and previous experimental data and CFD simulation data [7]
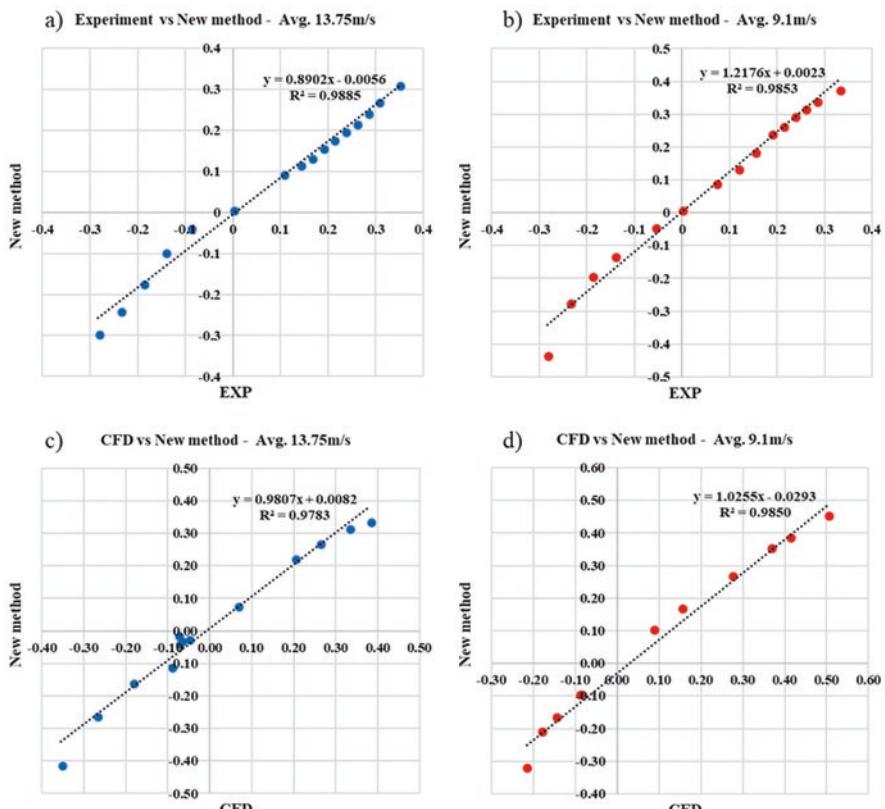
Fig. 12 Correlation of the new method with the (**a**, **b**) experimental data and (**c**, **d**) CFD simulation data for the average supply velocity of (**a**, **c**) 13.75 m/s case and (**b**, **d**) 9.1 m/s case

both the experimental and the CFD simulations, resulting in bigger discrepancies at this region. The R^2 coefficient of the 13.95 m/s cases are 0.989 and 0.978 for the experiment and the CFD results, respectively. For the 9.1 m/s cases, it is 0.985 and 0.985. In general, the high R^2 coefficient reflects the reliability of this new method.

5   Conclusions

A new approach to calculate the air curtain efficiency factor is established in this project by using a series of typical Q- ΔP curves. This provides an effective way to avoid complex experimental tests whereas at the same time to evaluate the effectiveness of air curtain products to reduce infiltration/exfiltration at building entrances under different ambient conditions, which only needs the measured data of air curtain velocity distribution and degradation following the ANSI/AMCA or ISO Standards. The typical Q- ΔP curves for 12 design scenarios are provided in the form of standard figures in this report for 3 discharge angles (0°, 10°, 20°), 2 nozzle depths (0.08 m and 0.10 m), and 2 door heights (2.4 m and 3 m). For the scenarios of doors higher than the door height of 3 m, an equivalent method based on the concept of the virtual air curtain unit is developed. The procedure to calculate the efficiency factor is demonstrated by the case studies of three off-the-shelf air curtain units.

Note that, the main logic of the proposed method is to identify the uniformity and the aerodynamic strength of the air curtain jet through the aerodynamic test and use the standard Q- ΔP curve figures to determine the infiltration/exfiltration rates through the air curtain door. For the successful application of the method, users should pay attention to the following tips.

1. In the aerodynamic test, the discharge angle of the air curtain should be 0°, based on which the jet theory equation for the inverse calculation of the discharge velocity was originally developed.
2. The measured data at the objective distance, which is preferred to be the door height, should be used for the inverse calculation of the discharge velocity.
3. When a design scenario (e.g., door height, jet velocity, or angle) is out of the scope of the provided standard figures, interpolations/extrapolations among the existing curves should be performed to obtain the closest results.
4. The proposed method is assumed to be applicable to non-isothermal and wind conditions, should the total pressure difference under both conditions include the stack and/or wind effects and can be obtained or measured, which may need to be further confirmed.

Finally, the proposed method is validated by the data from the previous studies, and a reasonable agreement of the results exhibits the validity of the method.

Appendices

Appendix A

Please note the y-axis is the q_i (originally defined in Eq. 6) with the unit of Pa$^{0.5}$: $q_i = Q_i / \left(A_i \sqrt{\dfrac{2}{\rho}} \right)$

The x-axis is the pressure difference ΔP with the unit of Pa (Figs. 13, 14, 15, 16, 17, 18, 19, 20, 21, 22, 23, and 24).

Appendix B

Please note the data in Appendix B is used for the generation of the standard curves in Appendix A (Tables 18, 19, 20, 21, 22, 23, 24, 25, 26, 27, 28, and 29).
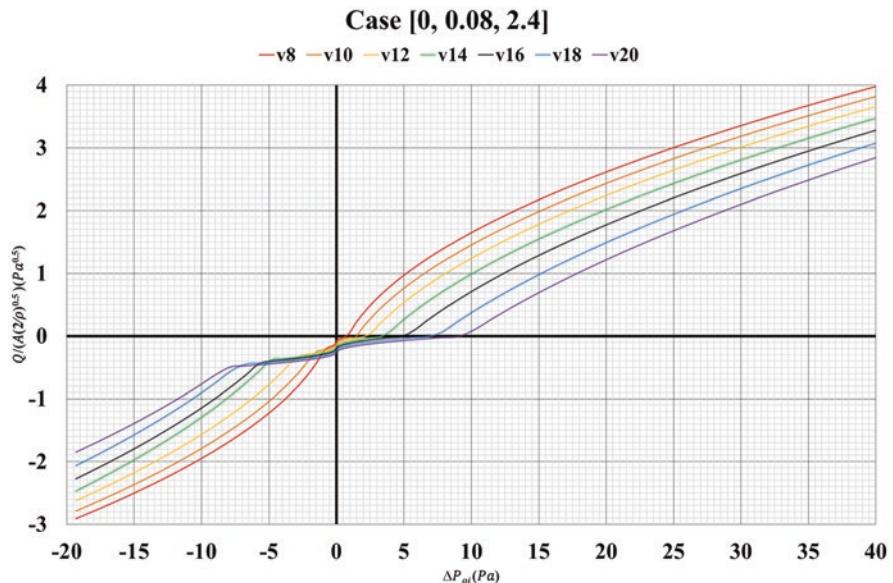
Fig. 13 The standard figure of the typical Q- ΔP curves for 2.4 m door, 0.08 m nozzle depth, and discharge angle of 0°
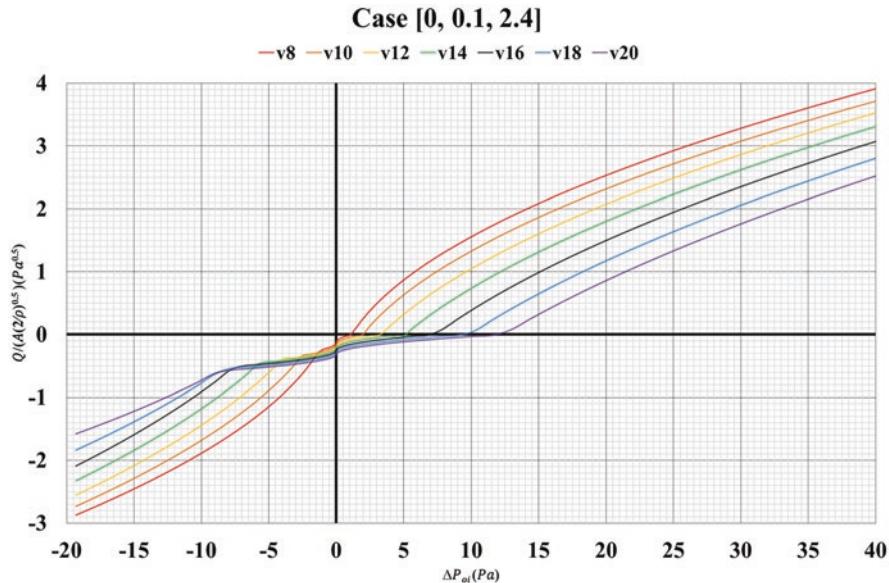
Fig. 14 The standard figure of the typical Q- ΔP curves for 2.4 m door, 0.1 m nozzle depth, and discharge angle of 0°
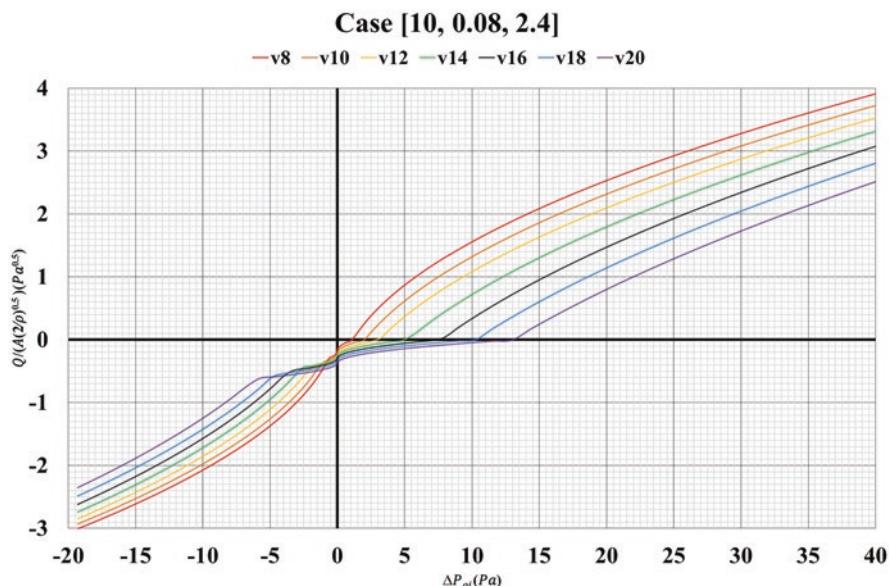
Fig. 15 The standard figure of the typical Q- ΔP curves for 2.4 m door, 0.08 m nozzle depth, and discharge angle of 10°
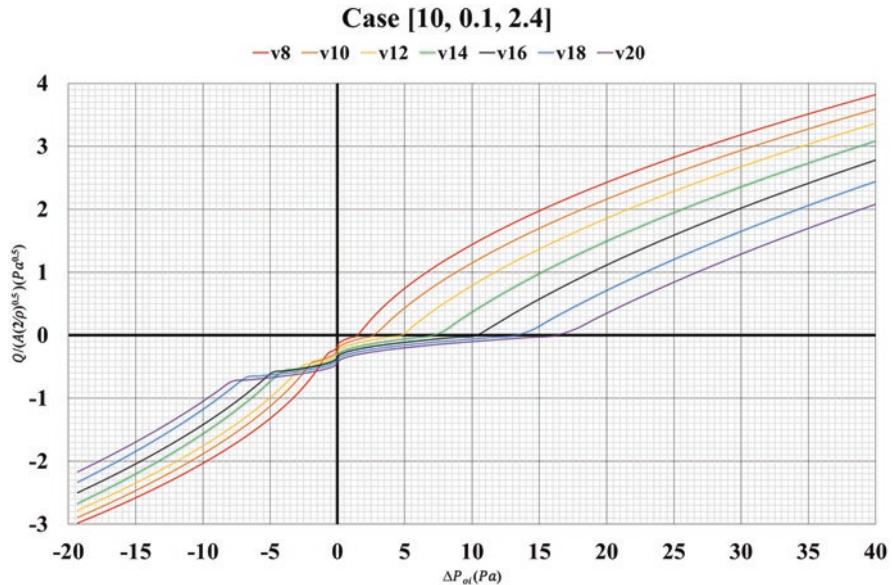
Fig. 16 The standard figure of the typical Q- ΔP curves for 2.4 m door, 0.1 m nozzle depth, and discharge angle of 10°

Fig. 17 The standard figure of the typical Q- ΔP curves for 2.4 m door, 0.08 m nozzle depth, and discharge angle of 20°

Case [20, 0.1, 2.4]
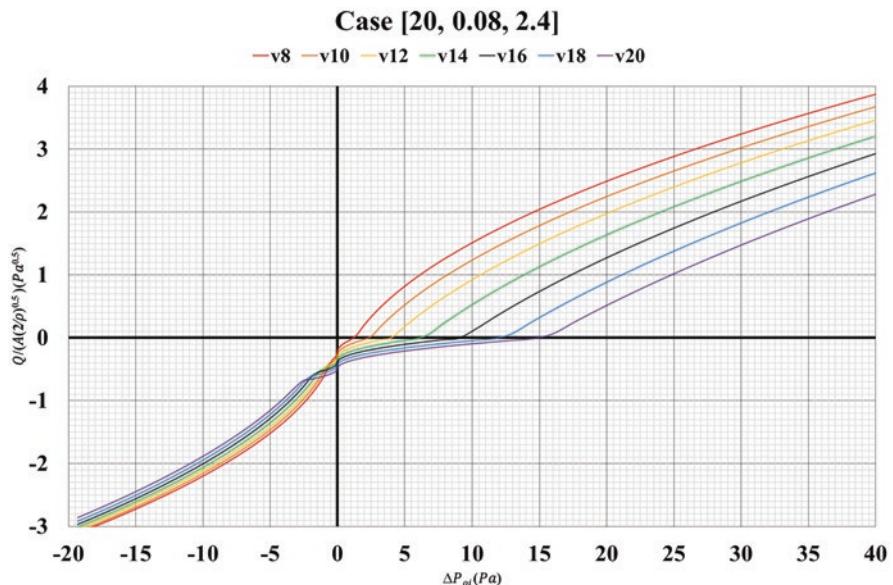
—v8 —v10 —v12 —v14 —v16 —v18 —v20

Fig. 18 The standard figure of the typical Q- ΔP curves for 2.4 m door, 0.1 m nozzle depth, and discharge angle of 20°

Case [0, 0.08, 3]
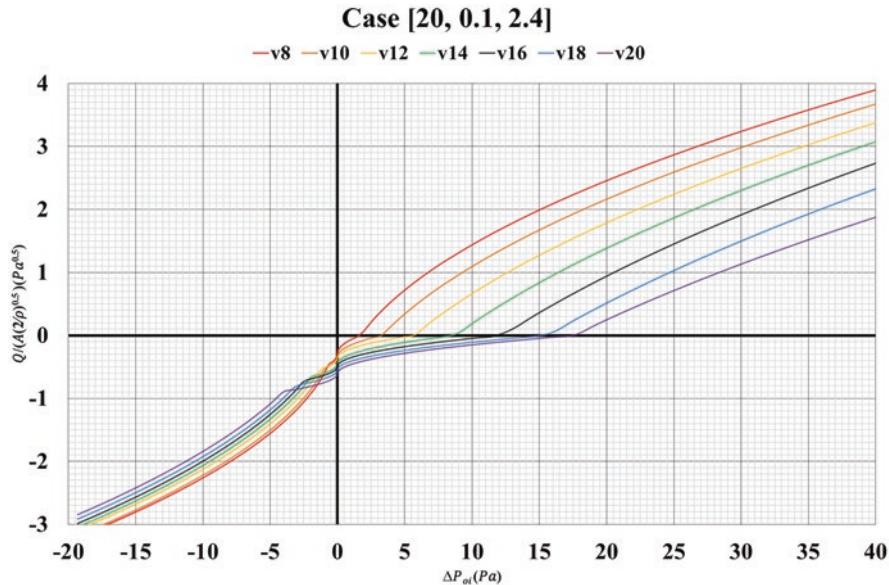
—v8 —v10 —v12 —v14 —v16 —v18 —v20
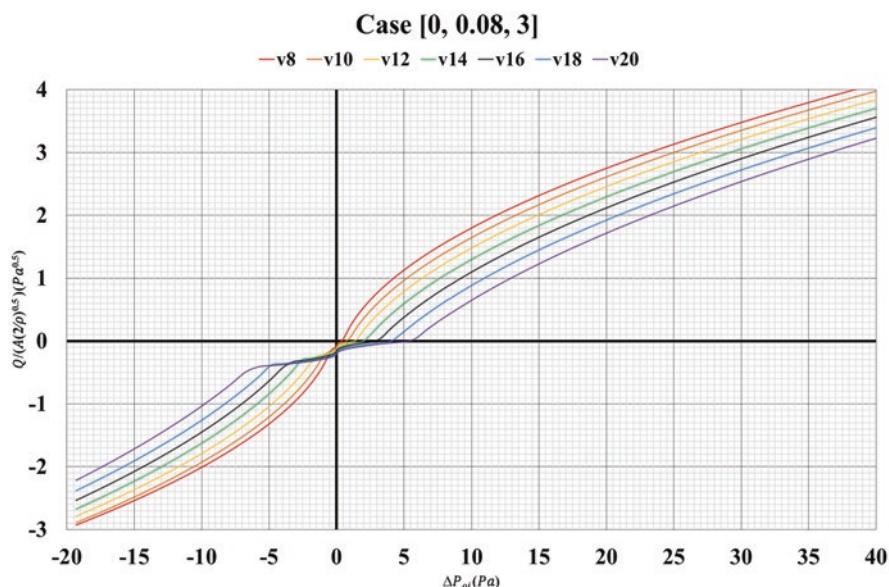
Fig. 19 The standard figure of the typical Q- ΔP curves for 3 m door, 0.08 m nozzle depth, and discharge angle of 0°
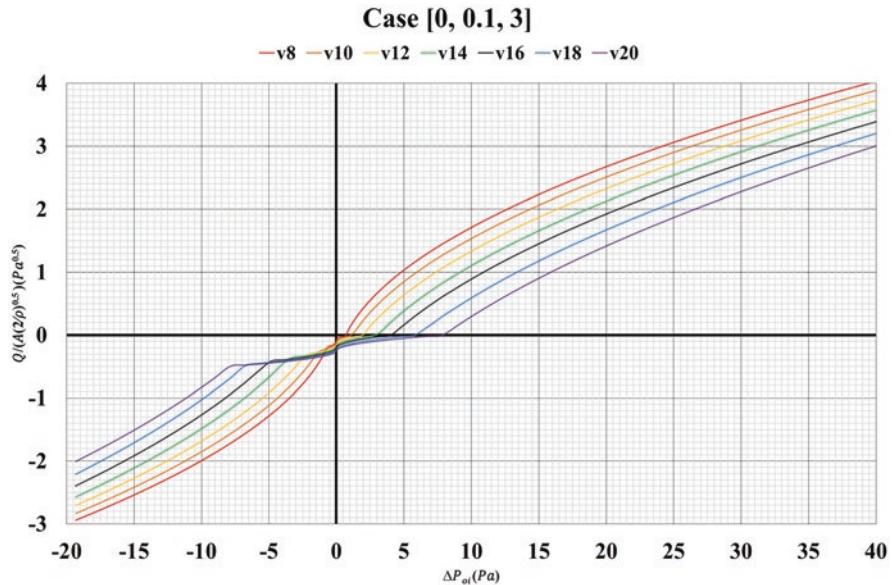
Fig. 20 The standard figure of the typical Q- ΔP curves for 3 m door, 0.1 m nozzle depth, and discharge angle of 0°
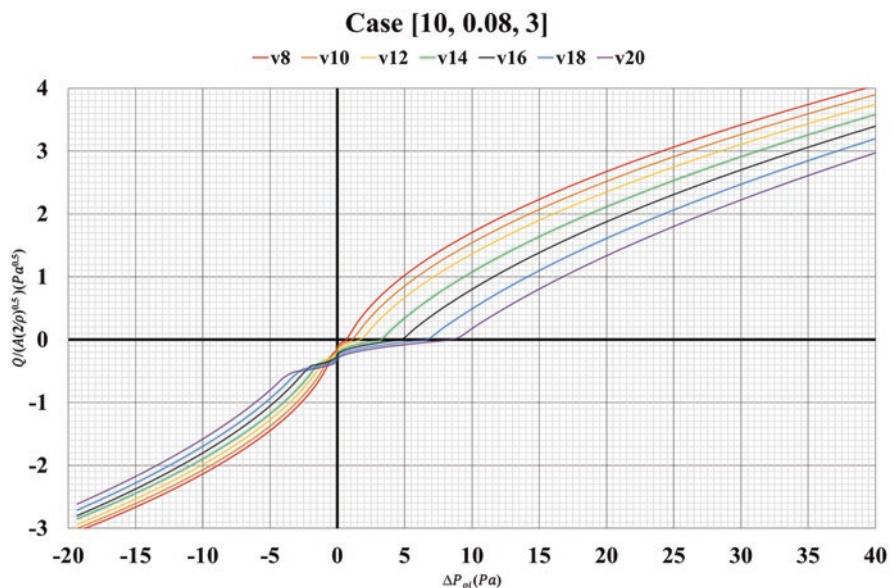
Fig. 21 The standard figure of the typical Q- ΔP curves for 3 m door, 0.08 m nozzle depth, and discharge angle of 10°
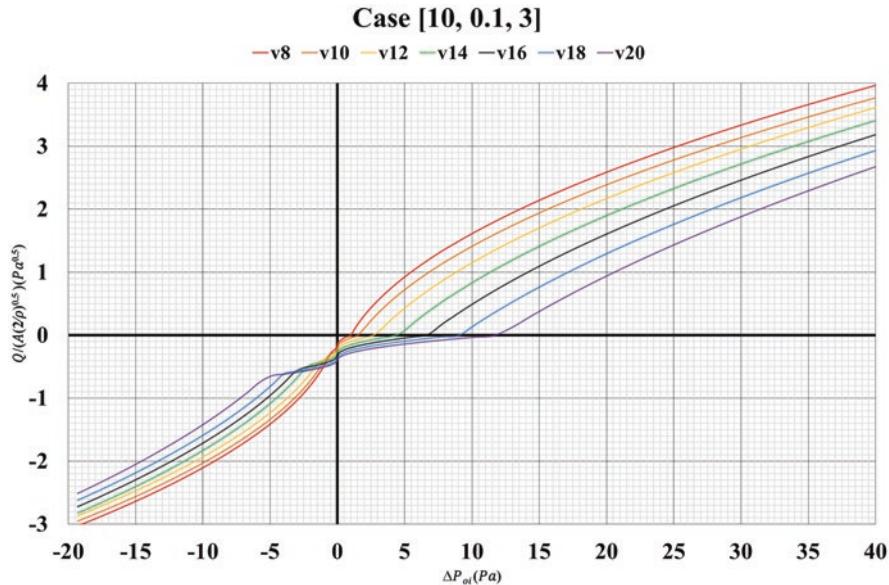
Fig. 22 The standard figure of the typical Q- ΔP curves for 3 m door, 0.1 m nozzle depth, and discharge angle of 10°
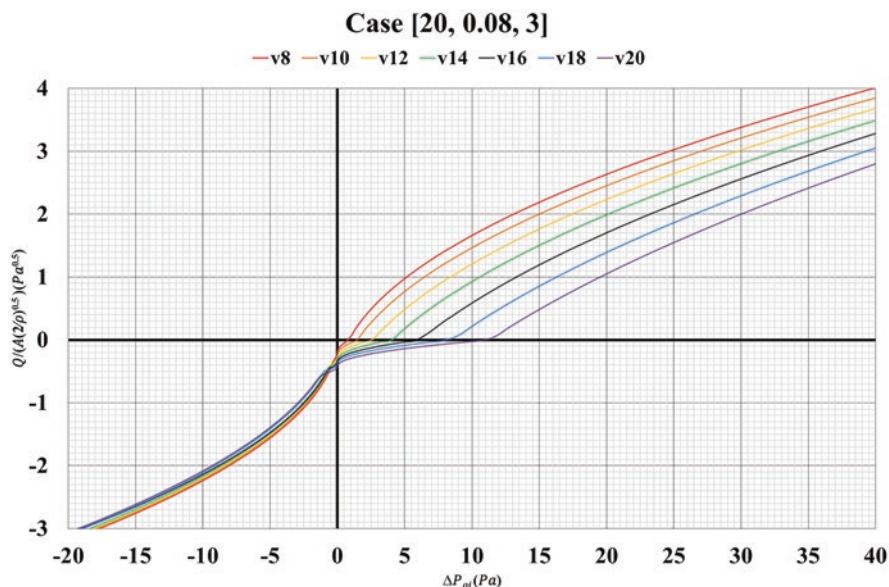
Fig. 23 The standard figure of the typical Q- ΔP curves for 3 m door, 0.08 m nozzle depth, and discharge angle of 20°
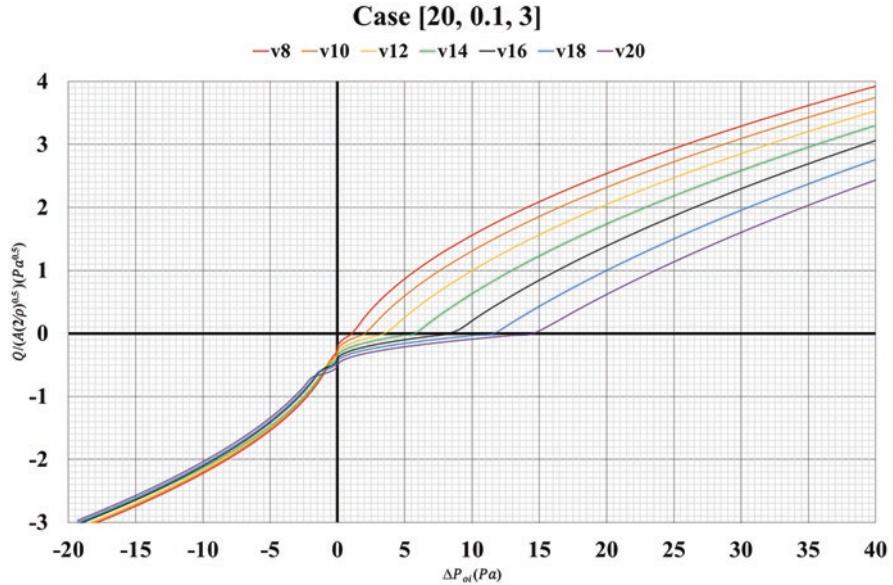
Fig. 24 The standard figure of the typical Q- ΔP curves for 3 m door, 0.1 m nozzle depth, and discharge angle of 20°

Table 18 Original data of the standard curves for 2.4 m door, 0.08 m nozzle depth, and discharge angle of 0°

ΔP Pa	8 m/s	10 m/s	12 m/s	14 m/s	16 m/s	18 m/s	20 m/s
40.96	4.03	3.87	3.71	3.53	3.34	3.14	2.91
38.44	3.88	3.72	3.56	3.38	3.18	2.97	2.73
36.00	3.74	3.57	3.41	3.22	3.02	2.80	2.56
33.64	3.59	3.42	3.25	3.06	2.85	2.62	2.38
31.36	3.44	3.27	3.10	2.90	2.69	2.45	2.21
29.16	3.29	3.12	2.95	2.75	2.53	2.28	2.03
27.04	3.15	2.97	2.80	2.59	2.37	2.11	1.86
25.00	3.00	2.83	2.64	2.43	2.20	1.94	1.68
23.04	2.85	2.68	2.49	2.28	2.04	1.77	1.51
21.16	2.71	2.53	2.34	2.12	1.88	1.60	1.33
19.36	2.56	2.38	2.19	1.96	1.72	1.43	1.15
17.64	2.41	2.23	2.03	1.81	1.55	1.26	0.98
16.00	2.26	2.08	1.88	1.65	1.39	1.09	0.80
14.44	2.12	1.93	1.73	1.49	1.23	0.92	0.63
12.96	1.97	1.78	1.57	1.33	1.06	0.74	0.45
11.56	1.82	1.63	1.42	1.18	0.90	0.57	0.28
10.24	1.68	1.48	1.27	1.02	0.74	0.40	0.10
9.00	1.53	1.33	1.12	0.86	0.58	0.23	−0.01
7.84	1.38	1.18	0.96	0.71	0.41	0.06	−0.02

(continued)

Table 18 (continued)

ΔP Pa	8 m/s	10 m/s	12 m/s	14 m/s	16 m/s	18 m/s	20 m/s
6.76	1.23	1.03	0.81	0.55	0.25	−0.01	−0.04
5.76	1.09	0.88	0.66	0.39	0.09	−0.03	−0.06
4.84	0.94	0.73	0.50	0.23	−0.01	−0.04	−0.07
4.00	0.79	0.58	0.35	0.08	−0.03	−0.06	−0.09
3.24	0.65	0.43	0.20	−0.01	−0.04	−0.08	−0.11
2.56	0.50	0.28	0.05	−0.03	−0.06	−0.10	−0.12
1.96	0.35	0.14	−0.01	−0.05	−0.08	−0.11	−0.14
1.44	0.20	−0.01	−0.03	−0.07	−0.10	−0.13	−0.16
1.00	0.06	−0.02	−0.05	−0.08	−0.12	−0.15	−0.17
0.64	−0.01	−0.04	−0.07	−0.10	−0.13	−0.16	−0.19
0.36	−0.03	−0.06	−0.09	−0.12	−0.15	−0.18	−0.21
0.16	−0.06	−0.08	−0.11	−0.14	−0.17	−0.20	−0.22
0.04	−0.08	−0.10	−0.13	−0.16	−0.19	−0.21	−0.24
0.00	−0.10	−0.12	−0.15	−0.18	−0.20	−0.23	−0.26
−0.04	−0.12	−0.15	−0.17	−0.20	−0.22	−0.25	−0.27
−0.16	−0.14	−0.17	−0.19	−0.21	−0.24	−0.27	−0.29
−0.36	−0.16	−0.19	−0.21	−0.23	−0.26	−0.28	−0.31
−0.64	−0.19	−0.21	−0.23	−0.25	−0.28	−0.30	−0.32
−1.00	−0.26	−0.23	−0.25	−0.27	−0.29	−0.32	−0.34
−1.44	−0.42	−0.25	−0.27	−0.29	−0.31	−0.33	−0.36
−1.96	−0.57	−0.36	−0.29	−0.31	−0.33	−0.35	−0.37
−2.56	−0.73	−0.52	−0.31	−0.33	−0.35	−0.37	−0.39
−3.24	−0.89	−0.69	−0.40	−0.34	−0.37	−0.38	−0.41
−4.00	−1.04	−0.85	−0.57	−0.36	−0.38	−0.40	−0.42
−4.84	−1.20	−1.01	−0.74	−0.38	−0.40	−0.42	−0.44
−5.76	−1.35	−1.17	−0.91	−0.56	−0.45	−0.44	−0.46
−6.76	−1.51	−1.33	−1.08	−0.76	−0.63	−0.45	−0.47
−7.84	−1.67	−1.50	−1.25	−0.95	−0.81	−0.56	−0.49
−9.00	−1.82	−1.66	−1.43	−1.14	−1.00	−0.75	−0.62
−10.24	−1.98	−1.82	−1.60	−1.33	−1.18	−0.94	−0.80
−11.56	−2.13	−1.98	−1.77	−1.52	−1.36	−1.13	−0.97
−12.96	−2.29	−2.14	−1.94	−1.71	−1.55	−1.32	−1.15
−14.44	−2.44	−2.31	−2.11	−1.90	−1.73	−1.51	−1.32
−16.00	−2.60	−2.47	−2.28	−2.09	−1.91	−1.69	−1.50
−17.64	−2.76	−2.63	−2.45	−2.28	−2.10	−1.88	−1.67
−19.36	−2.91	−2.79	−2.63	−2.47	−2.28	−2.07	−1.85

Table 19 Original data of the standard curves for 2.4 m door, 0.1 m nozzle depth, and discharge angle of 0°

ΔP Pa	8 m/s	10 m/s	12 m/s	14 m/s	16 m/s	18 m/s	20 m/s
40.96	3.96	3.77	3.58	3.37	3.13	2.87	2.59
38.44	3.82	3.62	3.43	3.21	2.97	2.70	2.41
36.00	3.67	3.47	3.27	3.04	2.80	2.52	2.23
33.64	3.52	3.32	3.11	2.88	2.63	2.34	2.05
31.36	3.37	3.17	2.96	2.72	2.46	2.17	1.87
29.16	3.22	3.02	2.80	2.55	2.29	1.99	1.69
27.04	3.07	2.87	2.64	2.39	2.12	1.82	1.52
25.00	2.92	2.72	2.49	2.23	1.95	1.64	1.34
23.04	2.77	2.57	2.33	2.07	1.78	1.47	1.16
21.16	2.63	2.42	2.17	1.90	1.61	1.29	0.98
19.36	2.48	2.27	2.02	1.74	1.44	1.11	0.80
17.64	2.33	2.12	1.86	1.58	1.27	0.94	0.62
16.00	2.18	1.96	1.70	1.42	1.10	0.76	0.44
14.44	2.03	1.81	1.55	1.25	0.93	0.59	0.26
12.96	1.88	1.66	1.39	1.09	0.76	0.41	0.08
11.56	1.73	1.51	1.23	0.93	0.59	0.23	−0.01
10.24	1.59	1.36	1.08	0.77	0.42	0.06	−0.03
9.00	1.44	1.21	0.92	0.60	0.25	−0.01	−0.05
7.84	1.29	1.06	0.76	0.44	0.08	−0.03	−0.06
6.76	1.14	0.91	0.61	0.28	−0.01	−0.05	−0.08
5.76	0.99	0.76	0.45	0.11	−0.03	−0.07	−0.10
4.84	0.84	0.61	0.29	−0.05	−0.05	−0.08	−0.12
4.00	0.69	0.46	0.14	−0.03	−0.07	−0.10	−0.14
3.24	0.54	0.31	0.00	−0.04	−0.08	−0.12	−0.15
2.56	0.40	0.16	−0.02	−0.06	−0.10	−0.14	−0.17
1.96	0.25	0.00	−0.04	−0.08	−0.12	−0.16	−0.19
1.44	0.10	−0.02	−0.06	−0.10	−0.14	−0.18	−0.21
1.00	−0.01	−0.04	−0.09	−0.12	−0.16	−0.19	−0.23
0.64	−0.03	−0.07	−0.11	−0.14	−0.18	−0.21	−0.24
0.36	−0.05	−0.09	−0.13	−0.16	−0.20	−0.23	−0.26
0.16	−0.08	−0.11	−0.15	−0.18	−0.22	−0.25	−0.28
0.04	−0.10	−0.13	−0.17	−0.20	−0.23	−0.27	−0.30
0.00	−0.12	−0.16	−0.19	−0.22	−0.25	−0.28	−0.31
−0.04	−0.15	−0.18	−0.21	−0.24	−0.27	−0.30	−0.33
−0.16	−0.17	−0.20	−0.23	−0.26	−0.29	−0.32	−0.35
−0.36	−0.19	−0.22	−0.25	−0.28	−0.31	−0.34	−0.37
−0.64	−0.22	−0.25	−0.27	−0.30	−0.33	−0.36	−0.39
−1.00	−0.24	−0.27	−0.29	−0.32	−0.35	−0.38	−0.40
−1.44	−0.31	−0.29	−0.31	−0.34	−0.37	−0.39	−0.42
−1.96	−0.47	−0.31	−0.33	−0.36	−0.38	−0.41	−0.44
−2.56	−0.63	−0.34	−0.35	−0.38	−0.40	−0.43	−0.46

Table 19 (continued)

ΔP Pa	8 m/s	10 m/s	12 m/s	14 m/s	16 m/s	18 m/s	20 m/s
−3.24	−0.79	−0.51	−0.38	−0.40	−0.42	−0.45	−0.48
−4.00	−0.95	−0.68	−0.40	−0.42	−0.44	−0.47	−0.49
−4.84	−1.11	−0.86	−0.57	−0.44	−0.46	−0.48	−0.51
−5.76	−1.27	−1.03	−0.75	−0.47	−0.48	−0.50	−0.53
−6.76	−1.43	−1.20	−0.93	−0.66	−0.50	−0.52	−0.55
−7.84	−1.59	−1.37	−1.11	−0.84	−0.56	−0.54	−0.57
−9.00	−1.75	−1.54	−1.29	−1.03	−0.75	−0.63	−0.62
−10.24	−1.91	−1.71	−1.47	−1.22	−0.95	−0.80	−0.75
−11.56	−2.07	−1.88	−1.65	−1.40	−1.14	−0.98	−0.89
−12.96	−2.23	−2.05	−1.84	−1.59	−1.33	−1.15	−1.03
−14.44	−2.39	−2.22	−2.02	−1.77	−1.52	−1.32	−1.17
−16.00	−2.55	−2.39	−2.20	−1.96	−1.71	−1.50	−1.30
−17.64	−2.71	−2.56	−2.38	−2.15	−1.90	−1.67	−1.44
−19.36	−2.87	−2.73	−2.56	−2.33	−2.09	−1.84	−1.58

Table 20 Original data of the standard curves for 2.4 m door, 0.08 m nozzle depth, and discharge angle of 10°

ΔP Pa	8 m/s	10 m/s	12 m/s	14 m/s	16 m/s	18 m/s	20 m/s
40.96	3.97	3.79	3.59	3.38	3.14	2.88	2.58
38.44	3.82	3.63	3.43	3.21	2.97	2.70	2.40
36.00	3.67	3.48	3.28	3.05	2.79	2.52	2.21
33.64	3.52	3.33	3.13	2.88	2.62	2.34	2.03
31.36	3.37	3.18	2.97	2.72	2.45	2.16	1.85
29.16	3.23	3.03	2.82	2.56	2.28	1.98	1.66
27.04	3.08	2.87	2.66	2.39	2.10	1.80	1.48
25.00	2.93	2.72	2.51	2.23	1.93	1.62	1.29
23.04	2.78	2.57	2.35	2.06	1.76	1.44	1.11
21.16	2.63	2.42	2.20	1.90	1.58	1.26	0.92
19.36	2.48	2.26	2.04	1.74	1.41	1.08	0.74
17.64	2.33	2.11	1.89	1.57	1.24	0.90	0.55
16.00	2.18	1.96	1.74	1.41	1.06	0.72	0.37
14.44	2.04	1.81	1.58	1.24	0.89	0.54	0.18
12.96	1.89	1.66	1.43	1.08	0.72	0.36	0.00
11.56	1.74	1.50	1.27	0.92	0.54	0.18	−0.02
10.24	1.59	1.35	1.12	0.75	0.37	0.00	−0.04
9.00	1.44	1.20	0.96	0.59	0.20	−0.02	−0.06
7.84	1.29	1.05	0.81	0.43	0.02	−0.04	−0.08
6.76	1.14	0.90	0.65	0.26	−0.02	−0.06	−0.10
5.76	0.99	0.74	0.50	0.10	−0.04	−0.08	−0.12
4.84	0.85	0.59	0.34	−0.01	−0.06	−0.10	−0.14
4.00	0.70	0.44	0.19	−0.03	−0.08	−0.12	−0.16

Table 20 (continued)

ΔP Pa	8 m/s	10 m/s	12 m/s	14 m/s	16 m/s	18 m/s	20 m/s
3.24	0.55	0.29	0.04	−0.05	−0.10	−0.15	−0.18
2.56	0.40	0.14	−0.02	−0.08	−0.12	−0.17	−0.20
1.96	0.25	0.00	−0.05	−0.10	−0.15	−0.19	−0.22
1.44	0.10	−0.03	−0.08	−0.12	−0.17	−0.21	−0.25
1.00	−0.01	−0.06	−0.10	−0.15	−0.19	−0.23	−0.27
0.64	−0.04	−0.09	−0.13	−0.17	−0.21	−0.25	−0.29
0.36	−0.07	−0.12	−0.16	−0.19	−0.23	−0.27	−0.31
0.16	−0.11	−0.15	−0.19	−0.21	−0.25	−0.29	−0.33
0.04	−0.14	−0.18	−0.21	−0.24	−0.27	−0.31	−0.35
0.00	−0.17	−0.21	−0.24	−0.26	−0.30	−0.33	−0.37
−0.04	−0.20	−0.24	−0.27	−0.28	−0.32	−0.35	−0.39
−0.16	−0.23	−0.27	−0.30	−0.30	−0.34	−0.37	−0.41
−0.36	−0.26	−0.29	−0.32	−0.33	−0.36	−0.39	−0.43
−0.64	−0.30	−0.32	−0.35	−0.35	−0.38	−0.41	−0.45
−1.00	−0.43	−0.35	−0.38	−0.37	−0.40	−0.43	−0.47
−1.44	−0.58	−0.45	−0.41	−0.39	−0.42	−0.46	−0.49
−1.96	−0.73	−0.61	−0.43	−0.42	−0.44	−0.48	−0.51
−2.56	−0.88	−0.76	−0.59	−0.44	−0.47	−0.50	−0.53
−3.24	−1.03	−0.92	−0.75	−0.58	−0.49	−0.52	−0.55
−4.00	−1.19	−1.07	−0.91	−0.75	−0.58	−0.54	−0.57
−4.84	−1.34	−1.23	−1.07	−0.92	−0.75	−0.59	−0.59
−5.76	−1.49	−1.38	−1.24	−1.08	−0.92	−0.77	−0.61
−6.76	−1.64	−1.54	−1.40	−1.25	−1.09	−0.94	−0.74
−7.84	−1.79	−1.69	−1.56	−1.41	−1.26	−1.11	−0.92
−9.00	−1.95	−1.85	−1.72	−1.58	−1.43	−1.28	−1.10
−10.24	−2.10	−2.00	−1.88	−1.75	−1.60	−1.46	−1.28
−11.56	−2.25	−2.16	−2.04	−1.91	−1.77	−1.63	−1.46
−12.96	−2.40	−2.31	−2.20	−2.08	−1.94	−1.80	−1.64
−14.44	−2.55	−2.47	−2.36	−2.24	−2.11	−1.97	−1.82
−16.00	−2.70	−2.62	−2.53	−2.41	−2.28	−2.15	−2.00
−17.64	−2.86	−2.78	−2.69	−2.58	−2.45	−2.32	−2.18
−19.36	−3.01	−2.93	−2.85	−2.74	−2.62	−2.49	−2.36

Table 21 Original data of the standard curves for 2.4 m door, 0.1 m nozzle depth, and discharge angle of 10°

ΔP Pa	8 m/s	10 m/s	12 m/s	14 m/s	16 m/s	18 m/s	20 m/s
40.96	3.88	3.65	3.43	3.15	2.85	2.51	2.15
38.44	3.73	3.50	3.26	2.98	2.67	2.33	1.97
36.00	3.58	3.34	3.10	2.81	2.49	2.14	1.78
33.64	3.43	3.19	2.94	2.63	2.31	1.95	1.59
31.36	3.28	3.03	2.77	2.46	2.13	1.76	1.40
29.16	3.13	2.88	2.61	2.29	1.95	1.58	1.22
27.04	2.98	2.72	2.45	2.12	1.77	1.39	1.03
25.00	2.83	2.57	2.29	1.95	1.59	1.20	0.84
23.04	2.68	2.42	2.12	1.78	1.41	1.02	0.66
21.16	2.53	2.26	1.96	1.60	1.23	0.83	0.47
19.36	2.38	2.11	1.80	1.43	1.05	0.64	0.28
17.64	2.23	1.95	1.63	1.26	0.87	0.46	0.10
16.00	2.07	1.80	1.47	1.09	0.69	0.27	−0.01
14.44	1.92	1.64	1.31	0.92	0.51	0.08	−0.03
12.96	1.77	1.49	1.15	0.75	0.33	−0.01	−0.05
11.56	1.62	1.34	0.98	0.57	0.15	−0.03	−0.07
10.24	1.47	1.18	0.82	0.40	0.00	−0.05	−0.10
9.00	1.32	1.03	0.66	0.23	−0.02	−0.08	−0.12
7.84	1.17	0.87	0.49	0.06	−0.05	−0.10	−0.14
6.76	1.02	0.72	0.33	−0.02	−0.07	−0.12	−0.16
5.76	0.87	0.56	0.17	−0.04	−0.09	−0.14	−0.18
4.84	0.72	0.41	0.01	−0.06	−0.11	−0.16	−0.20
4.00	0.57	0.25	−0.02	−0.09	−0.13	−0.18	−0.22
3.24	0.42	0.10	−0.05	−0.11	−0.15	−0.20	−0.24
2.56	0.27	−0.01	−0.07	−0.14	−0.18	−0.22	−0.26
1.96	0.12	−0.04	−0.10	−0.16	−0.20	−0.24	−0.29
1.44	−0.01	−0.07	−0.12	−0.18	−0.22	−0.27	−0.31
1.00	−0.03	−0.09	−0.15	−0.21	−0.24	−0.29	−0.33
0.64	−0.06	−0.12	−0.18	−0.23	−0.26	−0.31	−0.35
0.36	−0.09	−0.15	−0.20	−0.25	−0.28	−0.33	−0.37
0.16	−0.11	−0.18	−0.23	−0.28	−0.31	−0.35	−0.39
0.04	−0.14	−0.21	−0.25	−0.30	−0.33	−0.37	−0.41
0.00	−0.17	−0.23	−0.28	−0.33	−0.35	−0.39	−0.43
−0.04	−0.19	−0.26	−0.30	−0.35	−0.37	−0.41	−0.46
−0.16	−0.22	−0.29	−0.33	−0.37	−0.39	−0.43	−0.48
−0.36	−0.25	−0.32	−0.35	−0.40	−0.41	−0.46	−0.50
−0.64	−0.28	−0.35	−0.38	−0.42	−0.44	−0.48	−0.52
−1.00	−0.37	−0.37	−0.40	−0.45	−0.46	−0.50	−0.54
−1.44	−0.52	−0.40	−0.43	−0.47	−0.48	−0.52	−0.56
−1.96	−0.67	−0.44	−0.45	−0.49	−0.50	−0.54	−0.58
−2.56	−0.83	−0.60	−0.48	−0.52	−0.52	−0.56	−0.60

(continued)

Table 21 (continued)

ΔP Pa	8 m/s	10 m/s	12 m/s	14 m/s	16 m/s	18 m/s	20 m/s
−3.24	−0.98	−0.77	−0.63	−0.54	−0.54	−0.58	−0.63
−4.00	−1.14	−0.93	−0.79	−0.57	−0.57	−0.60	−0.65
−4.84	−1.29	−1.09	−0.96	−0.70	−0.59	−0.62	−0.67
−5.76	−1.44	−1.26	−1.12	−0.88	−0.75	−0.65	−0.69
−6.76	−1.60	−1.42	−1.29	−1.06	−0.92	−0.67	−0.71
−7.84	−1.75	−1.59	−1.46	−1.24	−1.10	−0.83	−0.73
−9.00	−1.91	−1.75	−1.62	−1.42	−1.27	−1.02	−0.90
−10.24	−2.06	−1.91	−1.79	−1.60	−1.45	−1.21	−1.08
−11.56	−2.22	−2.08	−1.95	−1.78	−1.62	−1.40	−1.26
−12.96	−2.37	−2.24	−2.12	−1.96	−1.80	−1.58	−1.45
−14.44	−2.52	−2.41	−2.29	−2.14	−1.97	−1.77	−1.63
−16.00	−2.68	−2.57	−2.45	−2.32	−2.15	−1.96	−1.81
−17.64	−2.83	−2.73	−2.62	−2.49	−2.32	−2.15	−1.99
−19.36	−2.99	−2.90	−2.78	−2.67	−2.50	−2.34	−2.17

Table 22 Original data of the standard curves for 2.4 m door, 0.08 m nozzle depth, and discharge angle of 20°

ΔP Pa	8 m/s	10 m/s	12 m/s	14 m/s	16 m/s	18 m/s	20 m/s
40.96	3.93	3.73	3.52	3.27	3.00	2.69	2.35
38.44	3.78	3.58	3.36	3.10	2.82	2.50	2.16
36.00	3.63	3.43	3.20	2.93	2.64	2.32	1.97
33.64	3.48	3.27	3.04	2.76	2.46	2.13	1.78
31.36	3.33	3.12	2.88	2.59	2.28	1.94	1.59
29.16	3.18	2.96	2.72	2.42	2.10	1.75	1.40
27.04	3.03	2.81	2.56	2.25	1.92	1.57	1.21
25.00	2.88	2.65	2.40	2.08	1.74	1.38	1.02
23.04	2.73	2.50	2.24	1.91	1.57	1.19	0.83
21.16	2.58	2.35	2.08	1.74	1.39	1.00	0.64
19.36	2.44	2.19	1.92	1.58	1.21	0.82	0.45
17.64	2.29	2.04	1.75	1.41	1.03	0.63	0.25
16.00	2.14	1.88	1.59	1.24	0.85	0.44	0.06
14.44	1.99	1.73	1.43	1.07	0.67	0.25	−0.02
12.96	1.84	1.58	1.27	0.90	0.49	0.07	−0.04
11.56	1.69	1.42	1.11	0.73	0.31	−0.02	−0.07
10.24	1.54	1.27	0.95	0.56	0.14	−0.04	−0.09
9.00	1.39	1.11	0.79	0.39	−0.01	−0.07	−0.12
7.84	1.24	0.96	0.63	0.22	−0.03	−0.09	−0.14
6.76	1.09	0.80	0.47	0.05	−0.06	−0.11	−0.17
5.76	0.94	0.65	0.31	−0.02	−0.08	−0.14	−0.19
4.84	0.79	0.50	0.15	−0.05	−0.11	−0.16	−0.21
4.00	0.64	0.34	0.00	−0.07	−0.14	−0.19	−0.24

(continued)

Table 22 (continued)

ΔP Pa	8 m/s	10 m/s	12 m/s	14 m/s	16 m/s	18 m/s	20 m/s
3.24	0.50	0.19	−0.03	−0.10	−0.16	−0.21	−0.26
2.56	0.35	0.03	−0.07	−0.13	−0.19	−0.24	−0.29
1.96	0.20	−0.03	−0.10	−0.16	−0.21	−0.26	−0.31
1.44	0.05	−0.06	−0.13	−0.19	−0.24	−0.29	−0.34
1.00	−0.03	−0.10	−0.16	−0.21	−0.26	−0.31	−0.36
0.64	−0.07	−0.13	−0.19	−0.24	−0.29	−0.34	−0.39
0.36	−0.11	−0.17	−0.22	−0.27	−0.32	−0.36	−0.41
0.16	−0.15	−0.20	−0.25	−0.30	−0.34	−0.39	−0.44
0.04	−0.19	−0.24	−0.29	−0.32	−0.37	−0.41	−0.46
0.00	−0.23	−0.27	−0.32	−0.35	−0.39	−0.43	−0.49
−0.04	−0.27	−0.31	−0.35	−0.38	−0.42	−0.46	−0.51
−0.16	−0.31	−0.34	−0.38	−0.41	−0.44	−0.48	−0.54
−0.36	−0.34	−0.38	−0.41	−0.43	−0.47	−0.51	−0.56
−0.64	−0.46	−0.41	−0.44	−0.46	−0.50	−0.53	−0.59
−1.00	−0.61	−0.53	−0.48	−0.49	−0.52	−0.56	−0.61
−1.44	−0.75	−0.68	−0.64	−0.55	−0.55	−0.58	−0.64
−1.96	−0.90	−0.83	−0.79	−0.71	−0.63	−0.61	−0.66
−2.56	−1.05	−0.98	−0.94	−0.86	−0.78	−0.71	−0.68
−3.24	−1.19	−1.13	−1.09	−1.02	−0.94	−0.87	−0.81
−4.00	−1.34	−1.28	−1.24	−1.17	−1.10	−1.03	−0.97
−4.84	−1.49	−1.43	−1.39	−1.32	−1.25	−1.19	−1.12
−5.76	−1.64	−1.58	−1.54	−1.48	−1.41	−1.34	−1.28
−6.76	−1.78	−1.73	−1.69	−1.63	−1.56	−1.50	−1.44
−7.84	−1.93	−1.88	−1.84	−1.78	−1.72	−1.66	−1.60
−9.00	−2.08	−2.03	−1.99	−1.94	−1.88	−1.82	−1.76
−10.24	−2.23	−2.18	−2.14	−2.09	−2.03	−1.97	−1.91
−11.56	−2.37	−2.33	−2.30	−2.25	−2.19	−2.13	−2.07
−12.96	−2.52	−2.49	−2.45	−2.40	−2.35	−2.29	−2.23
−14.44	−2.67	−2.64	−2.60	−2.55	−2.50	−2.45	−2.39
−16.00	−2.81	−2.79	−2.75	−2.71	−2.66	−2.60	−2.55
−17.64	−2.96	−2.94	−2.90	−2.86	−2.82	−2.76	−2.71
−19.36	−3.11	−3.09	−3.05	−3.01	−2.97	−2.92	−2.86

Table 23 Original data of the standard curves for 2.4 m door, 0.1 m nozzle depth, and discharge angle of 20°

ΔP Pa	8 m/s	10 m/s	12 m/s	14 m/s	16 m/s	18 m/s	20 m/s
40.96	3.96	3.73	3.44	3.14	2.81	2.40	1.94
38.44	3.80	3.57	3.27	2.96	2.61	2.20	1.77
36.00	3.65	3.41	3.10	2.78	2.42	2.01	1.59
33.64	3.49	3.24	2.93	2.60	2.23	1.81	1.42
31.36	3.33	3.08	2.75	2.41	2.03	1.62	1.24
29.16	3.18	2.92	2.58	2.23	1.84	1.42	1.07
27.04	3.02	2.75	2.41	2.05	1.65	1.22	0.89
25.00	2.87	2.59	2.24	1.87	1.45	1.03	0.71
23.04	2.71	2.43	2.07	1.68	1.26	0.83	0.54
21.16	2.56	2.26	1.90	1.50	1.07	0.64	0.36
19.36	2.40	2.10	1.73	1.32	0.87	0.44	0.19
17.64	2.25	1.94	1.55	1.14	0.68	0.25	0.01
16.00	2.09	1.78	1.38	0.96	0.49	0.05	−0.03
14.44	1.94	1.61	1.21	0.77	0.29	−0.02	−0.06
12.96	1.78	1.45	1.04	0.59	0.10	−0.05	−0.08
11.56	1.62	1.29	0.87	0.41	−0.01	−0.08	−0.11
10.24	1.47	1.12	0.70	0.23	−0.04	−0.10	−0.14
9.00	1.31	0.96	0.52	0.04	−0.07	−0.13	−0.17
7.84	1.16	0.80	0.35	−0.02	−0.10	−0.16	−0.20
6.76	1.00	0.63	0.18	−0.05	−0.13	−0.19	−0.23
5.76	0.85	0.47	0.01	−0.08	−0.15	−0.21	−0.26
4.84	0.69	0.31	−0.03	−0.11	−0.18	−0.24	−0.29
4.00	0.54	0.15	−0.06	−0.14	−0.21	−0.27	−0.32
3.24	0.38	0.00	−0.09	−0.17	−0.24	−0.30	−0.34
2.56	0.22	−0.04	−0.12	−0.20	−0.27	−0.33	−0.37
1.96	0.07	−0.08	−0.15	−0.23	−0.30	−0.35	−0.40
1.44	−0.02	−0.12	−0.18	−0.27	−0.32	−0.38	−0.43
1.00	−0.07	−0.15	−0.21	−0.30	−0.35	−0.41	−0.46
0.64	−0.11	−0.19	−0.24	−0.33	−0.38	−0.44	−0.49
0.36	−0.16	−0.23	−0.27	−0.36	−0.41	−0.46	−0.52
0.16	−0.20	−0.27	−0.30	−0.39	−0.44	−0.49	−0.55
0.04	−0.24	−0.30	−0.33	−0.42	−0.46	−0.52	−0.57
0.00	−0.29	−0.34	−0.36	−0.45	−0.49	−0.55	−0.60
−0.04	−0.33	−0.38	−0.39	−0.48	−0.52	−0.58	−0.63
−0.16	−0.38	−0.42	−0.42	−0.51	−0.55	−0.60	−0.66
−0.36	−0.42	−0.45	−0.45	−0.54	−0.58	−0.63	−0.69
−0.64	−0.46	−0.49	−0.48	−0.57	−0.61	−0.66	−0.72
−1.00	−0.61	−0.55	−0.52	−0.60	−0.63	−0.69	−0.75
−1.44	−0.77	−0.70	−0.60	−0.63	−0.66	−0.71	−0.78
−1.96	−0.92	−0.86	−0.75	−0.66	−0.69	−0.74	−0.80
−2.56	−1.07	−1.01	−0.91	−0.82	−0.74	−0.77	−0.83

Table 23 (continued)

ΔP Pa	8 m/s	10 m/s	12 m/s	14 m/s	16 m/s	18 m/s	20 m/s
−3.24	−1.22	−1.17	−1.06	−0.98	−0.90	−0.83	−0.86
−4.00	−1.38	−1.32	−1.22	−1.14	−1.06	−0.99	−0.89
−4.84	−1.53	−1.48	−1.38	−1.30	−1.22	−1.15	−1.06
−5.76	−1.68	−1.63	−1.53	−1.46	−1.39	−1.31	−1.22
−6.76	−1.83	−1.79	−1.69	−1.61	−1.55	−1.47	−1.38
−7.84	−1.99	−1.94	−1.84	−1.77	−1.71	−1.63	−1.54
−9.00	−2.14	−2.10	−2.00	−1.93	−1.87	−1.79	−1.71
−10.24	−2.29	−2.25	−2.16	−2.09	−2.03	−1.96	−1.87
−11.56	−2.44	−2.41	−2.31	−2.25	−2.19	−2.12	−2.03
−12.96	−2.60	−2.56	−2.47	−2.41	−2.35	−2.28	−2.20
−14.44	−2.75	−2.72	−2.62	−2.57	−2.51	−2.44	−2.36
−16.00	−2.90	−2.87	−2.78	−2.73	−2.67	−2.60	−2.52
−17.64	−3.06	−3.03	−2.94	−2.88	−2.83	−2.76	−2.68
−19.36	−3.21	−3.18	−3.09	−3.04	−2.99	−2.92	−2.85

Table 24 Original data of the standard curves for 3 m door, 0.08 m nozzle depth, and discharge angle of 0°

ΔP Pa	8 m/s	10 m/s	12 m/s	14 m/s	16 m/s	18 m/s	20 m/s
40.96	4.15	4.03	3.90	3.76	3.62	3.46	3.29
38.44	4.00	3.88	3.75	3.61	3.46	3.30	3.12
36.00	3.86	3.73	3.60	3.46	3.31	3.14	2.96
33.64	3.71	3.59	3.45	3.31	3.15	2.98	2.80
31.36	3.57	3.44	3.30	3.15	3.00	2.82	2.63
29.16	3.42	3.29	3.15	3.00	2.84	2.66	2.47
27.04	3.28	3.15	3.00	2.85	2.69	2.50	2.31
25.00	3.13	3.00	2.85	2.70	2.53	2.35	2.15
23.04	2.99	2.85	2.70	2.55	2.37	2.19	1.98
21.16	2.84	2.70	2.55	2.39	2.22	2.03	1.82
19.36	2.70	2.56	2.41	2.24	2.06	1.87	1.66
17.64	2.55	2.41	2.26	2.09	1.91	1.71	1.49
16.00	2.41	2.26	2.11	1.94	1.75	1.55	1.33
14.44	2.26	2.12	1.96	1.78	1.60	1.39	1.17
12.96	2.12	1.97	1.81	1.63	1.44	1.24	1.01
11.56	1.97	1.82	1.66	1.48	1.28	1.08	0.84
10.24	1.83	1.67	1.51	1.33	1.13	0.92	0.68
9.00	1.68	1.53	1.36	1.18	0.97	0.76	0.52
7.84	1.54	1.38	1.21	1.02	0.82	0.60	0.35
6.76	1.39	1.23	1.06	0.87	0.66	0.44	0.19
5.76	1.25	1.08	0.91	0.72	0.51	0.28	0.03
4.84	1.10	0.94	0.76	0.57	0.35	0.13	−0.01
4.00	0.96	0.79	0.61	0.42	0.19	0.00	−0.03

(continued)

Table 24 (continued)

ΔP Pa	8 m/s	10 m/s	12 m/s	14 m/s	16 m/s	18 m/s	20 m/s
3.24	0.81	0.64	0.46	0.26	0.04	−0.02	−0.05
2.56	0.67	0.50	0.32	0.11	−0.01	−0.04	−0.07
1.96	0.52	0.35	0.17	−0.01	−0.03	−0.06	−0.08
1.44	0.38	0.20	0.02	−0.02	−0.05	−0.08	−0.10
1.00	0.23	0.05	−0.02	−0.04	−0.07	−0.09	−0.12
0.64	0.09	−0.01	−0.04	−0.06	−0.09	−0.11	−0.13
0.36	−0.01	−0.03	−0.06	−0.08	−0.11	−0.13	−0.15
0.16	−0.03	−0.06	−0.08	−0.10	−0.13	−0.15	−0.17
0.04	−0.05	−0.08	−0.10	−0.12	−0.15	−0.16	−0.19
0.00	−0.07	−0.10	−0.12	−0.14	−0.16	−0.18	−0.20
−0.04	−0.09	−0.12	−0.14	−0.16	−0.18	−0.20	−0.22
−0.16	−0.11	−0.14	−0.16	−0.18	−0.20	−0.22	−0.24
−0.36	−0.13	−0.16	−0.18	−0.20	−0.22	−0.24	−0.25
−0.64	−0.25	−0.18	−0.20	−0.22	−0.24	−0.25	−0.27
−1.00	−0.39	−0.24	−0.22	−0.24	−0.26	−0.27	−0.29
−1.44	−0.54	−0.40	−0.24	−0.26	−0.28	−0.29	−0.31
−1.96	−0.69	−0.55	−0.36	−0.28	−0.29	−0.31	−0.32
−2.56	−0.84	−0.71	−0.52	−0.30	−0.31	−0.32	−0.34
−3.24	−0.99	−0.87	−0.68	−0.47	−0.33	−0.34	−0.36
−4.00	−1.14	−1.02	−0.85	−0.64	−0.43	−0.36	−0.37
−4.84	−1.29	−1.18	−1.01	−0.81	−0.60	−0.38	−0.39
−5.76	−1.44	−1.33	−1.17	−0.98	−0.78	−0.56	−0.41
−6.76	−1.59	−1.49	−1.33	−1.15	−0.95	−0.74	−0.50
−7.84	−1.74	−1.65	−1.49	−1.32	−1.13	−0.93	−0.69
−9.00	−1.89	−1.80	−1.66	−1.49	−1.31	−1.11	−0.88
−10.24	−2.04	−1.96	−1.82	−1.66	−1.48	−1.29	−1.07
−11.56	−2.19	−2.11	−1.98	−1.83	−1.66	−1.47	−1.26
−12.96	−2.34	−2.27	−2.14	−2.00	−1.84	−1.65	−1.45
−14.44	−2.49	−2.43	−2.30	−2.17	−2.01	−1.84	−1.65
−16.00	−2.63	−2.58	−2.47	−2.34	−2.19	−2.02	−1.84
−17.64	−2.78	−2.74	−2.63	−2.51	−2.36	−2.20	−2.03
−19.36	−2.93	−2.89	−2.79	−2.68	−2.54	−2.38	−2.22

Table 25 Original data of the standard curves for 3 m door, 0.1 m nozzle depth, and discharge angle of 0°

ΔP Pa	8 m/s	10 m/s	12 m/s	14 m/s	16 m/s	18 m/s	20 m/s
40.96	4.09	3.94	3.79	3.63	3.45	3.26	3.07
38.44	3.94	3.80	3.64	3.48	3.29	3.10	2.90
36.00	3.80	3.65	3.48	3.32	3.13	2.93	2.73
33.64	3.65	3.50	3.33	3.16	2.98	2.77	2.55
31.36	3.50	3.35	3.18	3.01	2.82	2.60	2.38
29.16	3.36	3.20	3.03	2.85	2.66	2.44	2.21
27.04	3.21	3.05	2.88	2.70	2.50	2.27	2.04
25.00	3.06	2.90	2.73	2.54	2.34	2.11	1.87
23.04	2.92	2.75	2.58	2.38	2.19	1.94	1.70
21.16	2.77	2.61	2.42	2.23	2.03	1.78	1.53
19.36	2.62	2.46	2.27	2.07	1.87	1.61	1.36
17.64	2.47	2.31	2.12	1.92	1.71	1.45	1.19
16.00	2.33	2.16	1.97	1.76	1.55	1.28	1.01
14.44	2.18	2.01	1.82	1.60	1.40	1.12	0.84
12.96	2.03	1.86	1.67	1.45	1.24	0.95	0.67
11.56	1.89	1.71	1.52	1.29	1.08	0.79	0.50
10.24	1.74	1.56	1.37	1.14	0.92	0.62	0.33
9.00	1.59	1.42	1.21	0.98	0.76	0.46	0.16
7.84	1.45	1.27	1.06	0.82	0.61	0.29	0.00
6.76	1.30	1.12	0.91	0.67	0.45	0.13	−0.02
5.76	1.15	0.97	0.76	0.51	0.29	0.00	−0.04
4.84	1.01	0.82	0.61	0.36	0.13	−0.02	−0.05
4.00	0.86	0.67	0.46	0.20	0.00	−0.04	−0.07
3.24	0.71	0.52	0.31	0.04	−0.02	−0.06	−0.09
2.56	0.57	0.37	0.16	−0.01	−0.04	−0.08	−0.11
1.96	0.42	0.23	0.00	−0.03	−0.06	−0.10	−0.12
1.44	0.27	0.08	−0.02	−0.05	−0.08	−0.12	−0.14
1.00	0.13	−0.01	−0.04	−0.07	−0.10	−0.13	−0.16
0.64	−0.02	−0.03	−0.06	−0.09	−0.12	−0.15	−0.18
0.36	−0.03	−0.06	−0.09	−0.12	−0.14	−0.17	−0.19
0.16	−0.05	−0.08	−0.11	−0.14	−0.16	−0.19	−0.21
0.04	−0.07	−0.10	−0.13	−0.16	−0.18	−0.21	−0.23
0.00	−0.10	−0.12	−0.15	−0.18	−0.20	−0.23	−0.25
−0.04	−0.12	−0.15	−0.17	−0.20	−0.22	−0.25	−0.27
−0.16	−0.14	−0.17	−0.19	−0.22	−0.24	−0.26	−0.28
−0.36	−0.17	−0.19	−0.21	−0.24	−0.26	−0.28	−0.30
−0.64	−0.19	−0.21	−0.24	−0.26	−0.28	−0.30	−0.32
−1.00	−0.33	−0.24	−0.26	−0.28	−0.30	−0.32	−0.34
−1.44	−0.49	−0.29	−0.28	−0.30	−0.32	−0.34	−0.35
−1.96	−0.64	−0.45	−0.30	−0.32	−0.34	−0.36	−0.37
−2.56	−0.79	−0.61	−0.39	−0.34	−0.36	−0.38	−0.39

(continued)

Table 25 (continued)

ΔP Pa	8 m/s	10 m/s	12 m/s	14 m/s	16 m/s	18 m/s	20 m/s
−3.24	−0.95	−0.77	−0.55	−0.36	−0.38	−0.39	−0.41
−4.00	−1.10	−0.93	−0.72	−0.46	−0.40	−0.41	−0.42
−4.84	−1.25	−1.09	−0.89	−0.64	−0.42	−0.43	−0.44
−5.76	−1.41	−1.25	−1.05	−0.81	−0.57	−0.45	−0.46
−6.76	−1.56	−1.41	−1.22	−0.99	−0.75	−0.49	−0.48
−7.84	−1.71	−1.56	−1.38	−1.16	−0.94	−0.68	−0.49
−9.00	−1.87	−1.72	−1.55	−1.34	−1.12	−0.87	−0.68
−10.24	−2.02	−1.88	−1.71	−1.52	−1.30	−1.06	−0.87
−11.56	−2.17	−2.04	−1.88	−1.69	−1.48	−1.25	−1.06
−12.96	−2.33	−2.20	−2.05	−1.87	−1.67	−1.44	−1.25
−14.44	−2.48	−2.36	−2.21	−2.04	−1.85	−1.64	−1.44
−16.00	−2.63	−2.52	−2.38	−2.22	−2.03	−1.83	−1.63
−17.64	−2.79	−2.68	−2.54	−2.40	−2.21	−2.02	−1.82
−19.36	−2.94	−2.84	−2.71	−2.57	−2.40	−2.21	−2.01

Table 26 Original data of the standard curves for 3 m door, 0.08 m nozzle depth, and discharge angle of 10°

ΔP Pa	8 m/s	10 m/s	12 m/s	14 m/s	16 m/s	18 m/s	20 m/s
40.96	4.10	3.95	3.80	3.64	3.46	3.26	3.04
38.44	3.95	3.80	3.65	3.48	3.29	3.09	2.86
36.00	3.80	3.65	3.50	3.32	3.13	2.92	2.69
33.64	3.66	3.50	3.35	3.17	2.96	2.75	2.51
31.36	3.51	3.36	3.20	3.01	2.80	2.57	2.33
29.16	3.36	3.21	3.05	2.85	2.64	2.40	2.16
27.04	3.21	3.06	2.90	2.69	2.47	2.23	1.98
25.00	3.06	2.91	2.74	2.53	2.31	2.06	1.80
23.04	2.92	2.76	2.59	2.37	2.14	1.89	1.62
21.16	2.77	2.61	2.44	2.21	1.98	1.72	1.45
19.36	2.62	2.46	2.29	2.06	1.82	1.55	1.27
17.64	2.47	2.31	2.14	1.90	1.65	1.38	1.09
16.00	2.33	2.17	1.99	1.74	1.49	1.21	0.92
14.44	2.18	2.02	1.84	1.58	1.32	1.04	0.74
12.96	2.03	1.87	1.69	1.42	1.16	0.87	0.56
11.56	1.88	1.72	1.54	1.26	0.99	0.69	0.39
10.24	1.73	1.57	1.39	1.10	0.83	0.52	0.21
9.00	1.59	1.42	1.24	0.95	0.67	0.35	0.03
7.84	1.44	1.27	1.09	0.79	0.50	0.18	−0.02
6.76	1.29	1.12	0.94	0.63	0.34	0.01	−0.04
5.76	1.14	0.97	0.79	0.47	0.17	−0.02	−0.06
4.84	1.00	0.83	0.64	0.31	0.01	−0.04	−0.08
4.00	0.85	0.68	0.49	0.15	−0.02	−0.07	−0.10

Table 26 (continued)

ΔP Pa	8 m/s	10 m/s	12 m/s	14 m/s	16 m/s	18 m/s	20 m/s
3.24	0.70	0.53	0.34	0.00	−0.05	−0.09	−0.13
2.56	0.55	0.38	0.19	−0.03	−0.07	−0.11	−0.15
1.96	0.41	0.23	0.04	−0.05	−0.09	−0.13	−0.17
1.44	0.26	0.08	−0.02	−0.08	−0.12	−0.16	−0.19
1.00	0.11	−0.01	−0.05	−0.10	−0.14	−0.18	−0.21
0.64	−0.01	−0.04	−0.08	−0.13	−0.16	−0.20	−0.23
0.36	−0.04	−0.07	−0.11	−0.15	−0.19	−0.22	−0.26
0.16	−0.07	−0.10	−0.14	−0.18	−0.21	−0.25	−0.28
0.04	−0.10	−0.13	−0.16	−0.21	−0.23	−0.27	−0.30
0.00	−0.13	−0.16	−0.19	−0.23	−0.26	−0.29	−0.32
−0.04	−0.16	−0.19	−0.22	−0.26	−0.28	−0.31	−0.34
−0.16	−0.19	−0.22	−0.25	−0.28	−0.30	−0.33	−0.37
−0.36	−0.23	−0.25	−0.28	−0.31	−0.33	−0.36	−0.39
−0.64	−0.38	−0.29	−0.31	−0.33	−0.35	−0.38	−0.41
−1.00	−0.53	−0.44	−0.34	−0.36	−0.38	−0.40	−0.43
−1.44	−0.68	−0.59	−0.48	−0.39	−0.40	−0.42	−0.45
−1.96	−0.82	−0.74	−0.63	−0.54	−0.42	−0.45	−0.47
−2.56	−0.97	−0.89	−0.79	−0.69	−0.54	−0.47	−0.50
−3.24	−1.12	−1.04	−0.94	−0.85	−0.70	−0.58	−0.52
−4.00	−1.27	−1.19	−1.10	−1.00	−0.87	−0.74	−0.61
−4.84	−1.42	−1.35	−1.25	−1.15	−1.03	−0.91	−0.78
−5.76	−1.57	−1.50	−1.40	−1.31	−1.19	−1.07	−0.94
−6.76	−1.72	−1.65	−1.56	−1.46	−1.35	−1.23	−1.11
−7.84	−1.86	−1.80	−1.71	−1.62	−1.51	−1.40	−1.28
−9.00	−2.01	−1.95	−1.86	−1.77	−1.67	−1.56	−1.45
−10.24	−2.16	−2.10	−2.02	−1.93	−1.83	−1.73	−1.61
−11.56	−2.31	−2.25	−2.17	−2.08	−2.00	−1.89	−1.78
−12.96	−2.46	−2.40	−2.33	−2.24	−2.16	−2.05	−1.95
−14.44	−2.61	−2.55	−2.48	−2.39	−2.32	−2.22	−2.12
−16.00	−2.76	−2.70	−2.63	−2.54	−2.48	−2.38	−2.28
−17.64	−2.90	−2.85	−2.79	−2.70	−2.64	−2.55	−2.45
−19.36	−3.05	−3.00	−2.94	−2.85	−2.80	−2.71	−2.62

Table 27 Original data of the standard curves for 3 m door, 0.1 m nozzle depth, and discharge angle of 10°

ΔP Pa	8 m/s	10 m/s	12 m/s	14 m/s	16 m/s	18 m/s	20 m/s
40.96	4.02	3.82	3.67	3.47	3.25	3.00	2.75
38.44	3.87	3.67	3.52	3.31	3.08	2.82	2.56
36.00	3.72	3.53	3.36	3.14	2.91	2.65	2.37
33.64	3.57	3.38	3.20	2.98	2.74	2.47	2.18
31.36	3.42	3.23	3.05	2.82	2.57	2.29	2.00
29.16	3.28	3.08	2.89	2.66	2.40	2.12	1.81
27.04	3.13	2.93	2.74	2.49	2.23	1.94	1.62
25.00	2.98	2.78	2.58	2.33	2.06	1.76	1.43
23.04	2.83	2.63	2.43	2.17	1.89	1.59	1.25
21.16	2.68	2.48	2.27	2.00	1.72	1.41	1.06
19.36	2.53	2.33	2.11	1.84	1.55	1.23	0.87
17.64	2.38	2.19	1.96	1.68	1.38	1.06	0.69
16.00	2.23	2.04	1.80	1.52	1.21	0.88	0.50
14.44	2.09	1.89	1.65	1.35	1.04	0.70	0.31
12.96	1.94	1.74	1.49	1.19	0.87	0.53	0.12
11.56	1.79	1.59	1.34	1.03	0.70	0.35	−0.01
10.24	1.64	1.44	1.18	0.87	0.53	0.17	−0.03
9.00	1.49	1.29	1.02	0.70	0.36	0.00	−0.05
7.84	1.34	1.14	0.87	0.54	0.19	−0.02	−0.08
6.76	1.19	0.99	0.71	0.38	0.02	−0.05	−0.10
5.76	1.05	0.84	0.56	0.21	−0.02	−0.07	−0.12
4.84	0.90	0.70	0.40	0.05	−0.05	−0.10	−0.14
4.00	0.75	0.55	0.25	−0.02	−0.07	−0.12	−0.17
3.24	0.60	0.40	0.09	−0.04	−0.10	−0.14	−0.19
2.56	0.45	0.25	−0.01	−0.07	−0.12	−0.17	−0.21
1.96	0.30	0.10	−0.04	−0.10	−0.15	−0.19	−0.23
1.44	0.15	−0.01	−0.07	−0.12	−0.17	−0.22	−0.26
1.00	0.00	−0.04	−0.10	−0.15	−0.20	−0.24	−0.28
0.64	−0.03	−0.07	−0.13	−0.18	−0.22	−0.26	−0.30
0.36	−0.06	−0.10	−0.16	−0.20	−0.25	−0.29	−0.32
0.16	−0.09	−0.13	−0.18	−0.23	−0.27	−0.31	−0.35
0.04	−0.13	−0.16	−0.21	−0.25	−0.30	−0.34	−0.37
0.00	−0.16	−0.20	−0.24	−0.28	−0.32	−0.36	−0.39
−0.04	−0.19	−0.23	−0.27	−0.31	−0.34	−0.38	−0.41
−0.16	−0.22	−0.26	−0.30	−0.33	−0.37	−0.41	−0.44
−0.36	−0.25	−0.29	−0.33	−0.36	−0.39	−0.43	−0.46
−0.64	−0.34	−0.32	−0.36	−0.39	−0.42	−0.45	−0.48
−1.00	−0.49	−0.41	−0.38	−0.41	−0.44	−0.48	−0.51
−1.44	−0.64	−0.56	−0.44	−0.44	−0.47	−0.50	−0.53
−1.96	−0.79	−0.71	−0.59	−0.46	−0.49	−0.53	−0.55
−2.56	−0.94	−0.86	−0.75	−0.57	−0.52	−0.55	−0.57

(continued)

Table 27 (continued)

ΔP Pa	8 m/s	10 m/s	12 m/s	14 m/s	16 m/s	18 m/s	20 m/s
−3.24	−1.09	−1.01	−0.90	−0.73	−0.60	−0.57	−0.60
−4.00	−1.23	−1.16	−1.05	−0.89	−0.76	−0.61	−0.62
−4.84	−1.38	−1.31	−1.20	−1.05	−0.92	−0.78	−0.64
−5.76	−1.53	−1.46	−1.35	−1.21	−1.09	−0.95	−0.74
−6.76	−1.68	−1.61	−1.51	−1.37	−1.25	−1.12	−0.92
−7.84	−1.83	−1.76	−1.66	−1.54	−1.41	−1.28	−1.10
−9.00	−1.98	−1.91	−1.81	−1.70	−1.58	−1.45	−1.27
−10.24	−2.13	−2.06	−1.96	−1.86	−1.74	−1.62	−1.45
−11.56	−2.28	−2.21	−2.11	−2.02	−1.91	−1.79	−1.63
−12.96	−2.43	−2.36	−2.26	−2.18	−2.07	−1.95	−1.81
−14.44	−2.58	−2.50	−2.42	−2.34	−2.23	−2.12	−1.98
−16.00	−2.73	−2.65	−2.57	−2.50	−2.40	−2.29	−2.16
−17.64	−2.88	−2.80	−2.72	−2.66	−2.56	−2.46	−2.34
−19.36	−3.03	−2.95	−2.87	−2.83	−2.72	−2.62	−2.52

Table 28 Original data of the standard curves for 3 m door, 0.08 m nozzle depth, and discharge angle of 20°

ΔP Pa	8 m/s	10 m/s	12 m/s	14 m/s	16 m/s	18 m/s	20 m/s
40.96	4.07	3.91	3.74	3.55	3.35	3.12	2.87
38.44	3.92	3.76	3.58	3.39	3.18	2.94	2.68
36.00	3.77	3.61	3.43	3.23	3.01	2.76	2.49
33.64	3.62	3.45	3.27	3.07	2.83	2.58	2.30
31.36	3.47	3.30	3.11	2.90	2.66	2.40	2.11
29.16	3.32	3.15	2.96	2.74	2.49	2.22	1.92
27.04	3.18	3.00	2.80	2.58	2.32	2.04	1.74
25.00	3.03	2.85	2.64	2.42	2.15	1.86	1.55
23.04	2.88	2.70	2.49	2.26	1.98	1.68	1.36
21.16	2.73	2.55	2.33	2.10	1.81	1.50	1.17
19.36	2.58	2.40	2.17	1.93	1.64	1.33	0.98
17.64	2.43	2.25	2.02	1.77	1.47	1.15	0.79
16.00	2.29	2.10	1.86	1.61	1.30	0.97	0.60
14.44	2.14	1.95	1.71	1.45	1.13	0.79	0.42
12.96	1.99	1.80	1.55	1.29	0.96	0.61	0.23
11.56	1.84	1.65	1.39	1.12	0.79	0.43	0.04
10.24	1.69	1.50	1.24	0.96	0.62	0.25	−0.02
9.00	1.54	1.35	1.08	0.80	0.45	0.07	−0.04
7.84	1.40	1.20	0.92	0.64	0.28	−0.02	−0.07
6.76	1.25	1.05	0.77	0.48	0.11	−0.04	−0.09
5.76	1.10	0.89	0.61	0.32	−0.01	−0.07	−0.12
4.84	0.95	0.74	0.46	0.15	−0.04	−0.09	−0.14
4.00	0.80	0.59	0.30	0.00	−0.07	−0.12	−0.17

Table 28 (continued)

ΔP Pa	8 m/s	10 m/s	12 m/s	14 m/s	16 m/s	18 m/s	20 m/s
3.24	0.65	0.44	0.14	−0.03	−0.09	−0.14	−0.19
2.56	0.51	0.29	0.00	−0.06	−0.12	−0.17	−0.22
1.96	0.36	0.14	−0.04	−0.09	−0.15	−0.20	−0.24
1.44	0.21	0.00	−0.07	−0.13	−0.18	−0.22	−0.27
1.00	0.06	−0.04	−0.11	−0.16	−0.21	−0.25	−0.29
0.64	−0.03	−0.08	−0.14	−0.19	−0.23	−0.27	−0.32
0.36	−0.07	−0.12	−0.17	−0.22	−0.26	−0.30	−0.34
0.16	−0.11	−0.16	−0.21	−0.25	−0.29	−0.32	−0.37
0.04	−0.16	−0.20	−0.24	−0.28	−0.32	−0.35	−0.39
0.00	−0.20	−0.24	−0.28	−0.31	−0.35	−0.38	−0.42
−0.04	−0.25	−0.28	−0.31	−0.34	−0.37	−0.40	−0.44
−0.16	−0.29	−0.32	−0.35	−0.37	−0.40	−0.43	−0.47
−0.36	−0.36	−0.36	−0.38	−0.40	−0.43	−0.45	−0.49
−0.64	−0.51	−0.47	−0.45	−0.43	−0.46	−0.48	−0.52
−1.00	−0.65	−0.62	−0.59	−0.56	−0.59	−0.51	−0.54
−1.44	−0.80	−0.76	−0.74	−0.71	−0.73	−0.64	−0.62
−1.96	−0.94	−0.91	−0.89	−0.86	−0.87	−0.79	−0.77
−2.56	−1.09	−1.06	−1.04	−1.01	−1.02	−0.94	−0.91
−3.24	−1.24	−1.21	−1.18	−1.16	−1.16	−1.09	−1.06
−4.00	−1.38	−1.35	−1.33	−1.30	−1.30	−1.24	−1.21
−4.84	−1.53	−1.50	−1.48	−1.45	−1.45	−1.39	−1.36
−5.76	−1.68	−1.65	−1.63	−1.60	−1.59	−1.54	−1.51
−6.76	−1.82	−1.80	−1.77	−1.75	−1.73	−1.69	−1.66
−7.84	−1.97	−1.95	−1.92	−1.90	−1.88	−1.84	−1.81
−9.00	−2.11	−2.09	−2.07	−2.04	−2.02	−1.99	−1.96
−10.24	−2.26	−2.24	−2.22	−2.19	−2.16	−2.14	−2.11
−11.56	−2.41	−2.39	−2.36	−2.34	−2.31	−2.29	−2.26
−12.96	−2.55	−2.54	−2.51	−2.49	−2.45	−2.44	−2.41
−14.44	−2.70	−2.68	−2.66	−2.64	−2.59	−2.59	−2.56
−16.00	−2.85	−2.83	−2.81	−2.79	−2.74	−2.74	−2.71
−17.64	−2.99	−2.98	−2.96	−2.93	−2.88	−2.89	−2.86
−19.36	−3.14	−3.13	−3.10	−3.08	−3.02	−3.04	−3.01

Table 29 Original data of the standard curves for 3 m door, 0.1 m nozzle depth, and discharge angle of 20°

ΔP Pa	8 m/s	10 m/s	12 m/s	14 m/s	16 m/s	18 m/s	20 m/s
40.96	3.98	3.80	3.59	3.37	3.13	2.83	2.51
38.44	3.83	3.65	3.43	3.20	2.95	2.64	2.31
36.00	3.68	3.49	3.27	3.03	2.77	2.45	2.12
33.64	3.53	3.34	3.11	2.86	2.59	2.26	1.92
31.36	3.38	3.19	2.95	2.69	2.41	2.07	1.72
29.16	3.23	3.03	2.79	2.52	2.23	1.88	1.53
27.04	3.08	2.88	2.63	2.35	2.05	1.69	1.33
25.00	2.93	2.72	2.47	2.18	1.87	1.50	1.14
23.04	2.78	2.57	2.31	2.01	1.69	1.31	0.94
21.16	2.63	2.42	2.15	1.85	1.50	1.12	0.74
19.36	2.48	2.26	1.99	1.68	1.32	0.93	0.55
17.64	2.34	2.11	1.83	1.51	1.14	0.74	0.35
16.00	2.19	1.95	1.67	1.34	0.96	0.55	0.16
14.44	2.04	1.80	1.51	1.17	0.78	0.36	−0.01
12.96	1.89	1.65	1.35	1.00	0.60	0.17	−0.03
11.56	1.74	1.49	1.19	0.83	0.42	0.00	−0.06
10.24	1.59	1.34	1.03	0.66	0.24	−0.03	−0.08
9.00	1.44	1.18	0.87	0.49	0.06	−0.06	−0.11
7.84	1.29	1.03	0.71	0.33	−0.02	−0.08	−0.14
6.76	1.14	0.88	0.55	0.16	−0.05	−0.11	−0.16
5.76	0.99	0.72	0.39	0.00	−0.08	−0.13	−0.19
4.84	0.84	0.57	0.23	−0.03	−0.10	−0.16	−0.22
4.00	0.69	0.42	0.07	−0.06	−0.13	−0.19	−0.24
3.24	0.54	0.26	−0.02	−0.09	−0.16	−0.21	−0.27
2.56	0.39	0.11	−0.05	−0.13	−0.19	−0.24	−0.30
1.96	0.24	−0.01	−0.09	−0.16	−0.22	−0.27	−0.32
1.44	0.09	−0.05	−0.12	−0.19	−0.25	−0.29	−0.35
1.00	−0.02	−0.09	−0.16	−0.22	−0.27	−0.32	−0.38
0.64	−0.06	−0.13	−0.19	−0.25	−0.30	−0.35	−0.40
0.36	−0.11	−0.17	−0.23	−0.28	−0.33	−0.37	−0.43
0.16	−0.15	−0.21	−0.26	−0.31	−0.36	−0.40	−0.45
0.04	−0.19	−0.25	−0.30	−0.34	−0.39	−0.43	−0.48
0.00	−0.24	−0.29	−0.33	−0.37	−0.42	−0.45	−0.51
−0.04	−0.28	−0.33	−0.36	−0.40	−0.44	−0.48	−0.53
−0.16	−0.33	−0.37	−0.40	−0.43	−0.47	−0.51	−0.56
−0.36	−0.37	−0.41	−0.43	−0.46	−0.50	−0.53	−0.59
−0.64	−0.49	−0.45	−0.47	−0.49	−0.53	−0.56	−0.61
−1.00	−0.63	−0.60	−0.57	−0.59	−0.56	−0.58	−0.64
−1.44	−0.78	−0.75	−0.71	−0.73	−0.63	−0.61	−0.67
−1.96	−0.93	−0.89	−0.86	−0.87	−0.78	−0.76	−0.71
−2.56	−1.07	−1.04	−1.01	−1.02	−0.93	−0.91	−0.86

(continued)

Table 29 (continued)

ΔP Pa	8 m/s	10 m/s	12 m/s	14 m/s	16 m/s	18 m/s	20 m/s
−3.24	−1.22	−1.19	−1.16	−1.16	−1.08	−1.05	−1.01
−4.00	−1.37	−1.34	−1.31	−1.30	−1.23	−1.20	−1.16
−4.84	−1.52	−1.48	−1.46	−1.45	−1.38	−1.35	−1.31
−5.76	−1.66	−1.63	−1.60	−1.59	−1.53	−1.50	−1.46
−6.76	−1.81	−1.78	−1.75	−1.73	−1.68	−1.65	−1.61
−7.84	−1.96	−1.93	−1.90	−1.88	−1.83	−1.80	−1.76
−9.00	−2.10	−2.07	−2.05	−2.02	−1.98	−1.95	−1.91
−10.24	−2.25	−2.22	−2.20	−2.16	−2.13	−2.10	−2.06
−11.56	−2.40	−2.37	−2.34	−2.31	−2.28	−2.25	−2.21
−12.96	−2.54	−2.52	−2.49	−2.45	−2.43	−2.40	−2.37
−14.44	−2.69	−2.66	−2.64	−2.59	−2.58	−2.55	−2.52
−16.00	−2.84	−2.81	−2.79	−2.74	−2.73	−2.70	−2.67
−17.64	−2.98	−2.96	−2.94	−2.88	−2.88	−2.85	−2.82
−19.36	−3.13	−3.11	−3.08	−3.02	−3.03	−3.00	−2.97

References

1. AMCA, *ANSI/AMCA Standard 220-05 Laboratory Methods of Testing Air Curtain Units for Aerodynamic Performance Rating* (Air Movement and Control Association International, Inc., Arlington Heights, 2012)
2. ASHRAE, *ASHRAE Handbook—HVAC Applications* (American Society of Heating, Refrigerating and Air Conditioning Engineers, Atlanta, 2015)
3. M.V. Belleghem et al., Heat transfer through vertically downward-blowing single-jet air curtains for cold rooms. Heat Transf. Eng. **33**, 1196–1206 (2012)
4. S. Goubran, D. Qi, W.F. Saleh, L.L. Wang, Comparing methods of modeling air infiltration through building entrances and their impact on building energy simulation. Energy Build. **138**, 579–590 (2017a)
5. S. Goubran, D. Qi, L.L. Wang Annual energy saving impact of air curtains in commercial reference buildings. Proceedings of ISHVAC-COBEE, Tianjin, China, 2015
6. S. Goubran, D. Qi, L.L. Wang, Assessing dynamic efficiency of air curtain in reducing whole building annual energy usage. Build. Simul. **10**, 497–507 (2017b)
7. S. Goubran, D. Qi, L.L. Wang, R. Zmeureanu, Experimental study on the flow characteristics of air curtains at building entrances. Build. Environ. **105**, 225–235 (2016)
8. H. Hammink, L. Hendriksen, Determination of the Climate Separation Efficiency of Biddle Air Curtains Doorflow HP-200 and Indac S200 under Laboratory Conditions, Netherland: Indac, S, 2011
9. F. Hayes, Heat transfer characteristics of the air curtain: A Plane jet subjected to transverse pressure and temperature gradients. PhD Thesis ed. s.l.: University of Illinois, USA, 1968
10. F.C. Hayes, W.F. Stoecker, Design data for air curtains. ASHRAE Trans. **75**(2), 168–180 (1969a)
11. F. Hayes, W. Stoecker, Heat transfer characteristics of the air curtain. ASHRAE Trans. **75**(2), 153–167 (1969b)
12. ISO, *ISO Standard 27327-1 Part 1 - Laboratory methods of testing for aerodynamic performance rating* (International Organization for Standardization, Geneva, 2009)
13. D. Qi, S. Goubran, L.L. Wang, R. Zumeureanu, Parametric study of air curtain door aerodynamics performance based on experiments and numerical simulations. Build. Environ. **129**, 65–73 (2018)

14. D. Qi, S. Goubran, R. Zmeureanu, L.L. Wang, Effect of People on Infiltration of Building Entrance with Air Curtains. Proceedings of ISHVAC-COBEE, Tianjin, China, 2015
15. L.L. Wang, Z. Zhong, An approach to determine infiltration characteristics of building entrance equipped with air curtains. Energy Build. **75**, 312–320 (2014a)
16. L.L. Wang, Z. Zhong, Whole building annual energy analysis of air curtain performance in commercial building. s.l., eSim, 2014b
17. G.K. Yuill, *Impact of high use automatic doors on infiltration* (ASHRAE, Atlanta, 1996)
18. G.K. Yuill, R. Upham, H. Chen, Air leakage through automatic doors. ASHRAE Trans. **106**(2), 145–160 (2000)